1   **New roads and challenges for fuel cells in heavy-duty transportation**
2

3   **Authors:**

4   David A. Cullen (*Center for Nanophase Materials Sciences, Oak Ridge National Laboratory,*
5   *Oak Ridge, TN, USA*), K.C. Neyerlin (*Chemistry and Nanoscience Center, National Renewable*
6   *Energy Laboratory, Golden, CO, USA*), Rajesh K. Ahluwalia (*Energy Systems Division,*
7   *Argonne National Laboratory, Lemont, IL, USA*), Rangachary Mukundan (*Materials Physics and*
8   *Applications Division, Los Alamos National Laboratory, Los Alamos, NM, USA*), Karren L.
9   More (*Center for Nanophase Materials Sciences, Oak Ridge National Laboratory, Oak Ridge,*
10   *TN, USA*), Rodney L. Borup (*Materials Physics and Applications Division, Los Alamos National*
11   *Laboratory, Los Alamos, NM, USA*), Adam Z. Weber (*Energy Storage and Distributed*
12   *Resources Division, Lawrence Berkeley National Laboratory, Berkeley, CA, USA*), Deborah J.
13   Myers (*Chemical Sciences and Engineering Division, Argonne National Laboratory, Lemont, IL,*
14   *USA*), and Ahmet Kusoglu (corresponding author: akusoglu@lbl.gov, *Energy Storage and*
15   *Distributed Resources Division, Lawrence Berkeley National Laboratory, Berkeley, CA, USA*)

16

17   **Abstract:**

18   The recent release of hydrogen economy roadmaps for several major countries emphasizes the
19   need for accelerated world-wide investment in research and development activities for hydrogen
20   production, storage, infrastructure, and utilization in transportation, industry, and the electrical
21   grid. Due to the high gravimetric energy density of hydrogen, the focus of technologies that
22   utilize this fuel has recently shifted from light-duty automotive to heavy-duty vehicle (HDV)
23   applications. Decades of development of cost-effective and durable polymer electrolyte
24   membrane fuel cells must now be leveraged to meet the increased efficiency and durability
25   requirements of the HDV market. This review summarizes the latest market outlooks and targets
26   for truck, bus, locomotive, and marine applications. Required changes to the fuel cell system and
27   operating conditions for meeting Class 8 long-haul truck targets are presented. The necessary
28   improvements in fuel cell materials and integration are also discussed against the benchmark of
29   current passenger fuel cell electric vehicles.

30

Interest in hydrogen as an energy carrier has been reinvigorated in recent years, driven by the need for more flexible utilization of renewable energy sources and increased security of the global energy market.[1] By 2050, hydrogen could meet 14% of the energy demand in US[2] and 24% of world's energy needs,[3] of which 30% is projected for use in transportation.[4] The hydrogen roadmap for Europe anticipates a potential to generate 25% of European Union energy demand from hydrogen by 2050 to mobilize a European fleet of over 50M fuel-cell vehicles.[4] Significant action has come from local and national governments, which are increasingly enacting legislation banning internal combustion engines (ICEs) in favor of electric vehicles (EVs). China, in particular, has drastically expanded its support of fuel cells, with a reported 2018 funding/subsidy level of ¥85 billion ($12.4 billion USD),[5] and Germany recently announced €9 billion ($10.2 billion USD) in funding for hydrogen and fuel cells.[6] The United States Department of Energy (US DOE) has supported fuel cell transportation R&D since the late 1970's, and their research and development targets to enable commercialization, including those of the Hydrogen at Scale (H2@Scale) initiative, have been widely cited.[7,8]

Polymer electrolyte membrane fuel cells (PEMFCs) have many benefits over conventional ICEs used in passenger light-duty vehicles (LDVs), including higher efficiencies (>60%), while providing similar driving range (> 300 miles) and fueling times (< 5 min). Fuel-cell electric vehicles (FCEVs) are in the early stages of commercialization, with approximately 7,000 sold or leased in the United States to date.[9] Nearly every major automotive manufacturer is developing FCEVs. However, the initial cost of these vehicles is not yet competitive, and current approaches to stack cost reduction can dramatically decrease the stack lifetime. Lack of hydrogen refueling stations and cost parity with gasoline are also significant constraints for widespread FCEV commercialization.

While fuel cells for LDVs have been in development for over two decades, heavy-duty applications have only recently attracted significant attention.[10] This shift has been catalyzed by the unique scalability of fuel cells in terms of both power and energy, which can be achieved by increasing the size of the fuel cell stack or hydrogen tank at a much smaller additional weight penalty than Li-ion batteries. Commercial deployment of HDVs also requires less infrastructure investment as fewer refueling stations are required due to dedicated and more predictable routes. However, the different drive cycles and operating conditions of heavy-duty vehicles (HDVs), as well as their significantly longer lifetimes, mean a substantial improvement in durability and a greater focus on fuel efficiency is required as compared to LDVs. For instance, over 75% of LDV miles are used for non-interstate travel, while 55% of truck travel is spent on interstate roads (bts.gov). Further, the average Class 8 trucks travels 6 times further than the average LDV.[11] The US in particular has a large industry relying on HDVs that exceeded 300 billion annual vehicle miles traveled (AMT) in 2018, of which over 180 billion was attributed to long-haul trucking.[2,12] The heavy-duty market is also a critical market for reducing energy consumption and emissions, as medium- and heavy-duty trucks consume 25% of the total annual vehicle fuel use and produce 23% of the total CO_2 emissions in the US today.[13,14] Furthermore, annual freight truck miles traveled is projected to increase by 54% by 2050.[15]

Herein, we review the recent roadmaps, market outlooks, and targets for FCEVs, with a focus on applications in the HDV sector. Taking on the specific case of Class 8 long-haul trucks, simulated drive cycles are presented which inform system level strategies for achieving the high efficiency and durability operation required by this application. An increase in operating cell voltage is presented as the most viable path forward to improved efficiency, with key changes in

76   system design proposed to address high power operation where the majority of fuel is consumed.
77   The materials and electrode design breakthroughs required for this new operating paradigm are
78   discussed in detail. A shift in focus to end-of-life performance is emphasized in the development
79   of advanced catalysts and supports, high-temperature membranes and ionomers, novel electrode
80   designs, and durable gas diffusion layers and bipolar plates. Finally, the materials utilized in the
81   Toyota Mirai passenger FCEV are presented as a benchmark for materials development and
82   innovation.

Emerging transportation markets for FCEVs

84   The substantial decrease in Li-ion battery cost and their introduction into various vehicle
85   markets, as well as increased electrification of the transportation sector, have resulted in a rapid
86   expansion of electrochemical transportation technologies.[16] While current fuel-cell and battery
87   LDV costs are estimated to be close to parity for similar driving,[17] the lack of a hydrogen fueling
88   infrastructure has severely limited the adoption of fuel cells for LDVs. An exception to the
89   implementation of PEMFCs is the material handling sector, where the central refueling nature of
90   these applications coupled with cost and operation advantages have allowed this technology to
91   be implemented without subsidies.[18] Working from that model, PEMFCs are increasingly being
92   examined for use in HDV applications where there is a need for high power and reduced
93   emissions, such as in ports for drayage or delivery vehicles with well-defined routes. Equally as
94   important are HDV applications that can benefit from the separation of energy storage and power
95   output, the inherent strength of fuel cell systems. Factoring in refueling time advantages and the
96   intrinsic power density, PEMFCs have significant performance advantages for both medium-
97   duty (MDV) and HDV applications.[19] Until recently, HDV applications utilizing PEMFCs have
98   primarily been limited to fuel-cell buses which have been employed by various US transit
99   authorities since the early 2000s. The fuel and battery system lifetimes in these applications
100   have exceeded 30,000 hours, with an average of 13,236 hours.[20] Much like their LDV
101   counterparts, buses have seen limited adoption due to both the high initial capital cost (>$1M)
102   and the scarcity of hydrogen fueling stations. However, these barriers are being lowered thanks
103   to a mix of government investment towards production of less expensive hydrogen, expanded
104   policies focused on increased electrification, and continuous technological advancements. This
105   progress is evident in the ever-expanding number of bus and truck fleet demonstration projects,
106   especially in Europe and China.[21]

107   In a roadmap to a US hydrogen economy developed by the Fuel Cell & Hydrogen Energy
108   Association (FCHEA), an ambitious plan from early scale-up in 2025 to broad roll out in 2030
109   could result in a 17M-ton demand for hydrogen with over 5600 fueling stations. In such a
110   scenario, the number of FCEVs is expected to dramatically increase to 200,000 in 2025 and
111   5.3M in 2030 for passenger cars and commercial vehicles.[2] The hydrogen roadmap for Europe
112   includes a 2030 market penetration of 45,000 HDVs and projects, by 2050, 1.7M HDVs (trucks
113   and buses) and 5000 trains.[4] Similarly, Japan projects the use of 1200 buses by 2030
114   (www.iphe.net/japan) and the Republic of Korea projects 70,000 trucks and buses by 2040
115   (www.iphe.net/republic-of-korea).

116   Similar opportunities are emerging for fuel cells for freight, regional, and switcher locomotives
117   due primarily to the tightening standards for NO_x, SO_x, particulates, and noise. Freight
118   locomotives consume a significant amount of fuel at high notch levels where the diesel engine is
119   most efficient, while yard switchers operate at idle and low notch levels where fuel cells are most
120   efficient. Depending on the service route, suburban passenger trains have frequent start-stops and

121 acceleration events. Preliminary indication is that fuel cells can have a 30-35% efficiency
122 advantage over diesel engines in freights and regionals, but >75% in yard switchers.[21] Durability
123 is a major challenge since the required engine lifetime is 10-15 years, 35,000 operating hours,
124 and ~3.6M miles.[22]

125 Fuel cells are also being considered for maritime applications primarily due to the International
126 Maritime Organization's ambition to cut sulfur emissions by 86% and CO_2 emissions by 50% by
127 2050.[5] Preliminary indication is that the efficiency advantage of fuel cells over marine diesel
128 engines may be small for medium and large container ships, although the emission advantages
129 are much greater. Again, durability is a major challenge since the required engine lifetime for
130 container ships is 25 years and 75,000-100,000 operating hours.[23]

131 These emerging fuel cell applications are summarized in **Figure 1**, which depicts the
132 significance and implication of the shift from LDV to HDV applications both in terms of size
133 and mileage driven. The dramatic increase in the average daily and lifetime mileage of these
134 applications shifts the focus from capital to operating costs (*CapEx* to *OpEx*). At the cell level,
135 this signals a switch from the current LDV focus on low Pt-loaded electrodes and very high
136 power densities to new material and integration solutions that will mitigate degradation and
137 increase efficiency. The following sections explore the case for long-haul HDV trucks, but the
138 same approach, challenges, and solutions are relevant to the other HDV applications.

139

140 **System strategies for increased efficiency and durability**

141 The recently-released DOE targets for hydrogen Class 8 long-haul trucks (**Figure 2**) emphasize
142 the longer lifetimes and increased efficiency demands of HDV applications, with nearly a four-
143 fold increase in system lifetime to a total of 12 years and 1M miles of operation.[24] For LDVs,
144 PEMFC peak efficiencies have reached approximately 65%, a significant gain over the tank-to-
145 wheels efficiency of gasoline-powered passenger vehicles around 19%. Such efficiency
146 advantages at 25% rated power will be harder to come by for MDV/HDVs, where diesel trucks
147 routinely obtain 40% efficiency at much higher rated powers of 50-100%.

148

149 These enhanced targets offer some distinct differences and opportunities for PEMFC design.
150 The specific materials and system requirements are determined by the drive cycle, which can
151 differ significantly even within a given application.[25,26] For example, the drive cycle for a Class 8
152 truck illustrated in **Figure 3a** is just one of three under consideration by the EPA's Greenhouse
153 Gas Emissions Model (GEM2).[27,28] The PEMFC voltages corresponding to this drive cycle were
154 simulated by the system modeling team at Argonne National Laboratory assuming a minimum
155 idle power of 20kW to limit the peak cathode potential, a strategy implemented to limit cathode
156 catalyst degradation.[29]

157

158 **Figure 3b** also illustrates how the system efficiency at rated power is dramatically affected by
159 the cell voltage and coolant temperature. For example, a stack operated at 0.675V (comparable to
160 current LDV operation at rated power) would need to run above 90°C to reject waste heat and
161 enables efficiencies of 43-46%. Efficiencies $\geq$ 50% can only be reached by operating above
162 0.7V. Higher voltages also allow lower operating temperatures that extend the durability of
163 electrodes and membranes. This modeling illustrates one of the difficulties encountered in HDV
164 operation: heat rejection at low speeds on steep gradients where the battery needs to be used to

165 supplement the PEMFC power. This hybrid strategy has also been used to limit the cell voltage
166 of the stack to 0.9V, as illustrated in the drive cycle in **Figure 3a**.
167

168 As noted in Fig. 3b, heat rejection in HDVs is facilitated by higher cell voltage at rated power,
169 which translates to lower power densities and bulkier stacks, and elevated operating temperatures
170 for smaller radiator fans (less parasitic power). Initial total cost of ownership analysis of Class-8
171 trucks also favors selection of higher cell voltage at rated power for higher efficiency (better fuel
172 economy) and higher permissible Pt loadings (initial capital cost). Since HDVs require extended
173 lifetime (25,000 h), the issue of durability is equally, if not more, critical. Thus, some of the
174 high-payoff material development related areas of research are a) high activity catalysts without
175 the restriction of very low PGM loadings, b) catalysts and ionomers stable at temperatures above
176 90-100°C, c) highly stable ionomers and membranes under dry conditions, and d) high durability
177 catalysts, catalyst supports, and membranes, which are discussed in detail in the materials
178 strategies section. The strategies for engineered solutions include limiting peak potentials in
179 drive cycles transients, and hybridization with a battery to idle stacks during periods of low
180 power demand. Implementing these strategies requires complete understanding of the
181 relationship between stack and membrane degradation rates and operating conditions (potential,
182 temperature, relative humidity) and the methods of controlling them. Voltage optimization in
183 LDVs focused on decreasing the overall ohmic and mass-transport resistances in a push towards
184 higher current densities. For the HDV space, the increased voltage and temperature requirements
185 for higher efficiencies require a more dedicated focus on reducing kinetic losses, mixed
186 potentials due to crossover hydrogen and oxygen, and localized issues due to catalyst/ionomer
187 interactions in the MEA, as discussed later. The specific mix of materials- and system-mitigation
188 strategies will need to be tailored to the stressors identified in the drive-cycle analysis and
189 specific hybridization strategy.

190 In terms of durability concerns, cell reversal can occur during unprotected startup-shutdown
191 transients and during fuel starvation resulting in the oxidation of the catalyst-carbon support.[30-32]
192 There has been extensive research to develop more stable supports, but solely materials solutions
193 have thus far been inadequate and engineering approaches of preventing formation of an H_2/air
194 front by depleting oxygen from the cathode during shutdown have proven more successful as
195 discussed in Box 1. Furthermore, voltage clipping is an effective mitigation strategy for limiting
196 carbon corrosion and catalyst particle coalescence during operation, and systems-level mitigation
197 strategies such as limiting upper and/or lower cell voltage (*i.e.*, cathode potential) have also been
198 investigated to prevent catalyst dissolution.[33,34] This strategy appears to have been implemented
199 in the current generation of PEMFC LDVs, but has the drawback of restricting the minimum
200 power that the system is allowed to generate, thus limiting overall system efficiency. Operating
201 at air flow rates only slightly higher than those needed for the required stack power (*i.e.*, high
202 oxygen utilization) and lower oxygen concentrations are some of the available options to expand
203 the operating power window by reducing the allowable idling power.
204

205 Another durability issue is ice formation when starting from subfreezing temperatures, which can
206 lead to electrode delamination and other performance losses arising from water-management-
207 related transport resistances. Many patents are available on approaches to prevent ice formation.
208 These include operating at low voltages (*i.e.*, low cathode potentials) during cold start to
209 maximize in-stack heat production to warm the stack above 0°C rapidly, which comes at the
210 expense of overall system efficiency, or purging the stack during shutdown at subfreezing

5

211   temperatures to remove liquid water and dehumidify the MEA.[35,36] An additional concern arising
212   from the extended HDV lifetime is the cumulative effect of contaminants introduced into the
213   MEA through the fuel stream, air stream, or from other components in the PEMFC stack or
214   balance of plant. There are numerous studies and reviews on this topic describing the poisoning
215   mechanisms and mitigation strategies.[37] The fuel and air purity requirements for HDV
216   applications are not expected to be any different from LDV applications, with increased Pt
217   loading offsetting the increasing durability requirements of HDVs. However, contaminants such
218   as iron, that could potentially lead to enhanced membrane degradation, are of great concern in
219   HDV applications and should be avoided until more robust membranes are synthesized or
220   mitigation strategies that either prevent the migration of contaminant ions to the membrane or
221   eliminate their degrading effects are developed.

222

Materials strategies for increased efficiency and durability

224   Many of the fundamental LDV durability limitations and failure mechanisms will be exacerbated
225   by the longer lifetime and potentially higher operating temperatures of HDV systems. New
226   operating, materials, and materials integration strategies are needed to address these challenges.
227   Possible means to address these challenges while also meeting lifetime and efficiency
228   requirements are hierarchical assemblies, optimized catalyst/support interactions, alternative
229   support or composite materials, chemically-modified membranes, tuned membrane/electrode
230   interfaces, and self-healing or hybrid ionomers. These concepts are discussed by MEA
231   component (**Figure 4**) in the following sections.

Catalyst and supports

233   The development of durable cathode oxygen reduction reaction (ORR) catalysts that minimize or
234   eliminate the use of Pt is a particularly active research area that has been summarized in recent
235   reviews.[38-41] While immense progress has been made in improving the activity and durability of
236   low and non-Pt ORR electrocatalysts, further improvements and significant R&D effort,
237   especially in the area of durability, are needed for these materials to be considered for the interim
238   target of 25,000 h for HDV applications.[38,41]

239   Fortunately, the shift in balance between capital and operating costs means the requirement for
240   ultralow loadings of precious metal catalysts (<0.125 mg cm^{-2}) for LDVs are not as critical
241   during the initial transition to HDVs, allowing for loadings around 0.3 mg cm^{-2}. Considering
242   fleet size and the current use of noble metals in Class 8 trucks for catalytic converters and
243   particulate filters; replacing diesel HDVs with FC-HDVs should not pose a significant increase
244   in Pt demand.

245   However, due to the extended lifetime and potentially higher operating temperatures of HDV
246   stacks, many of the same concerns remain or are exacerbated regarding loss of catalyst
247   electrochemically-active surface area (ECSA),[42-46] and the resulting loss of catalyst performance
248   and stack power density and system efficiency (*i.e.*, increase in voltage loss at a given current
249   density). The loss of ECSA is driven by Pt dissolution with subsequent deposition of the Pt in the
250   membrane[47] and redeposition of Pt onto existing particles (termed Ostwald ripening) and/or
251   particle coalescence.[39,48-52] It is noteworthy that platinum dissolution is especially prevalent
252   during potential cycling in the 0.6 to 0.95 V range, and thus is a concern for the cathode catalyst
253   and not a major concern for the anode catalyst, which operates at close to the reversible

254 hydrogen potential.   Recent work suggests catalyst particle-size distribution plays a more
255 significant role than overall particle size in mitigating ECSA loss via Ostwald ripening.
256 However, monodispersed catalyst particles are difficult to produce and the development of
257 scalable, cost-effective synthesis routes is an area particularly worthy of further research.[53]

258 In addition to tailoring particle size and dispersion, the ORR activity of Pt can be enhanced
259 through alloying with transition metals (TMs), such as Co and Ni. Despite pre-treatment of Pt-
260 TM alloys to remove leachable TM, additional leaching occurs during MEA assembly and
261 operation causing loss of the enhancing effects of the TM on ORR activity. [42,43,54]   In current
262 LDV systems, like that of the Toyota Mirai, the TM content of the cathode catalyst is only ~ 10
263 at.% and system controls are employed that limit the highest potential experienced by the
264 cathode to prevent TM loss during operation, while still allowing use of a catalyst with a higher
265 ORR activity than that of Pt.[55,56] In addition to performance penalties due to the impact of loss of
266 TM on ORR activity, dissolved TMs can also affect the proton and oxygen transport properties
267 of the ionomer in the cathode catalyst layer, thus further decreasing high-current-density
268 performance.[57] Thus, the longer lifetime requirements for HDV MEAs compared to those of
269 LDVs will present a significant challenge for alloy catalysts. **Figure 5** illustrates this challenge
270 by comparing the *beginning-of-life* (BOL) and *end-of-life* (EOL) performance of MEAs
271 composed of a commercial PtCo alloy or Pt cathode catalyst with similar average particle size
272 and distribution.   These two cells were subjected to the accelerated stress test (AST)
273 recommended by the US Department of Energy, which typically comprises 30,000 cathode
274 potential cycles between 0.6 and 0.95 V with 3 s holds at each potential, which has been shown
275 to equate to a projected system lifetime of 5,000 h.[7] Since the system lifetimes for HDV
276 applications are expected to be >25,000 h, the number of AST cycles was extended from 30,000
277 to 75,000. While the PtCo alloy-containing MEA does show improved BOL performance at low
278 current densities, this advantage is lost over the period of the test with the EOL performance of
279 the two catalysts being almost identical at the lower current densities (**Figure 5**). This durability
280 issue of current commercial alloy catalysts, combined with the inferior performance of alloy
281 catalysts at higher current densities due to mass-transport losses, is a significant issue that must
282 be addressed prior to implementation in HDVs.[43] There are several synthetic routes and
283 structures for Pt-based catalysts that have shown improved retention of TM and thus better
284 ability to maintain ORR activity and performance over time. One of the most promising
285 strategies is the use of Pt-TM intermetallics for which stability is imparted by the ordered
286 arrangement of Pt and TM in the catalyst particles.[38,58,59] Recently, there have been single-cell
287 lab-scale demonstrations showing improved TM and activity retention with ordered Pt-Co, Pt-Ni,
288 and Pt-Fe intermetallics with TM contents as high as 27 at%.

289

290 Increased attention is also being given to the carbon support structure, which plays a critical role
291 in catalyst particle size, dispersion, and interaction with the ionomer, as well as catalyst
292 durability. The geometry of the support's pores as well as the location of the catalyst particles
293 with respect to the pores impacts oxygen transport, ORR kinetics, and ECSA loss due to reduced
294 particle coalescence.[60] Carbon supports vary from highly-graphitized, corrosion-resistant carbons
295 with low porosity to the generally-favored higher surface area (HSA), but less stable,
296 mesoporous carbons, which show improved mass activity and accessibility to particles to
297 oxygen.[61] In particular, electrocatalysts with high mass activities (>600 mA/mg$_{Pt}$) have been

298 almost exclusively supported on porous carbons, where the location of Pt and Pt alloys within the
299 carbon pores prevents interaction with ionomer that could otherwise impede ORR kinetics.

300 While system-level strategies, such as depleting oxygen from the cathode during shut-down can
301 significantly mitigate the corrosion of the HSA mesoporous carbon supports, the longer HDV
302 lifetimes will require the development of catalyst and support combinations with low catalyst
303 particle mobility, lower extent of poisoning by ionomer, and inherent resistance of both catalyst
304 and support to corrosion. There has been extensive research to develop supports that are more
305 stable and that interact more strongly with catalyst particles to inhibit mobility. These include
306 oxides of refractory metals, carbides, nitrides, nitrogen-doped carbons, and graphitized
307 carbons.[62,63] To date, alternative materials to carbon have suffered from either insufficient BOL
308 electronic conductivity, loss of conductivity during operation, and/or low surface area and poor
309 Pt particle dispersion. While graphitized carbons have been shown to decrease carbon corrosion,
310 they also have lower surface areas than non-graphitized supports and thus suffer from issues with
311 adequately dispersing the catalyst particles and maintaining the dispersion. Promising
312 approaches for overcoming this conundrum include doping the graphitized supports with
313 elements, such as nitrogen, that strongly interact and anchor the catalyst particles.[64] Other novel
314 approaches include deposition of metal oxide, such as zirconia or silica, or carbon overlayers to
315 protect and stabilize the Pt particles against dissolution and migration and coalescence.[65-67]

316 A final key consideration is the benchmarking of catalyst activity and durability. The aqueous
317 electrolyte thin-film rotating disk electrode technique (TF-RDE) is an efficient way to screen
318 catalysts and develop structure-property relationships,[68] but the exceptional mass activities
319 observed in RDE rarely translate to high performance in MEAs, and, in many cases, even fall
320 short of the performance of baseline materials.[38] This not only emphasizes the need to consider
321 support effects in catalyst development, but also the stability of materials in the MEA vs.
322 aqueous environment[69] and the effects of electrode structure on catalyst performance, discussed
323 in following sections. Consequently, while novel catalysts with high mass activities are still of
324 interest,[70] HDV requirements necessitate a shift in focus towards durable catalyst-support
325 combinations, with evaluation and reporting including EOL performance in MEA, rather than
326 just BOL ORR activity in an aqueous environment.

327 **Ionomers and Membranes**

328 Ionomers are used as the ion-conducting solid-electrolyte in PEFCs, where they play a dual role
329 of both the proton-exchange membrane (PEM) separator that facilitates ion transport between the
330 electrodes, as well as the electrolyte binder in the CLs, where it provides percolated ion-
331 conduction pathway and binds the supported catalyst particles.[75,90] Within the CL, catalyst
332 ionomers exist as nanometer-thick electrolyte "thin films" that allow for reactant gas and water
333 transport in addition to proton conductivity. Ionomer properties within the CL can deviate
334 significantly from bulk membrane ones and are highly dependent on the interactions with the rest
335 of the CL constituents and are discussed in a later section below. Thus, performance and
336 durability requirements in fuel cells necessitate optimized ionomer multi-functionalities tailored
337 for PEM and CLs.

338 As a PEM, membrane chemical-mechanical stability becomes even more critical for HDVs due
339 to the longer required lifetime, higher operating temperatures, and the importance of minimizing
340 hydrogen and oxygen crossover for higher efficiencies. In addition, new degradation
341 mechanisms could emerge in HDVs over timescales that were previously not assessed in LDVs,

8

including a much longer period of exposure of other system components that can induce new or accelerated degradation pathways (such as iron ions acting as Fenton's reagents). Membranes for LDVs are based on perfluorinated sulfonic acid (PFSA) ionomer chemistry. PFSA-based membranes are the current state-of-the-art due to their ability to combine high ionic conductivity and inherent chemical-mechanical stability owing to their fluorocarbon chemistry. Ionomers with hydrocarbon-based random and block-co-polymers have also been investigated for PEMFC applications, resulting in ionomers that can exhibit conductivity comparable to that of PFSAs, however their long-term durability in a cell has not yet been demonstrated. While some hydrocarbon ionomers allow for reduced cost as well as tailored structures with a wider range of equivalent weight (inverse of the ion-exchange capacity) that can be tuned for transport, the challenge remains of meeting both mechanical toughness (to withstand the humidity cycling during operation) and chemical stability (to survive cell operation) requirements in a single material.[71,72] State-of-the-art PFSA membranes are mechanically supported, usually with an intra-membrane reinforcement, and chemically, with dopants, such as oxides of cerium and manganese, to scavenge the radicals that are known to attack the ionomers.[34,73] These radical scavengers, however, are mobile and readily move into the cathode at operating potentials and can result in performance losses.[34] In addition to additives, side-chain modifications as well as pretreatment and processing effects could provide additional parameters and tunability in membrane design.[71,73-77] Membrane thickness could become another design parameter for simultaneous optimization of performance and durability. This is in light of the increased emphasis on durability and fuel cost, making issues such as local non-uniformities, hydrogen and oxygen crossover, Ce depletion and mobility, and reinforcement strategies more important and requiring a different optimization function compared to LDVs discussed elsewhere.[34]

In addition, higher temperature operation, near or above 100°C, requires different operating strategies as higher humidification becomes untenable due to the need for pressurization, thereby necessitating novel, high-temperature membranes that maintain conductivity at lower relative humidity. Another important area is the exploration of the effect of other components on membrane durability, such as bipolar plates (through corrosion and leaching of TMs), cathode-catalyst layers (via interface misalignment and interactions), and gas-diffusion-layer (GDL) structure (through penetration by carbon fibers), even though some of these could be ameliorated using system-design strategies. Improved understanding of the effects of air contaminants, component leaching, radical scavenger migration, or any new additives that may be present in the hybrid membranes will be critical for improving membrane durability.

Electrode structure

An increase in cathode electrode performance will be necessary to achieve the MEA-level ORR mass activities required (>1 A/mg$_{Pt}$) and enable the high efficiencies that would yield cost savings vs. conventional diesel engines. Approaches to improving performance at high potentials include modifying the carbon support structure, manipulating support/catalyst interactions as mentioned above, and tailoring ionomer/ORR catalyst interactions either through material or integration strategies (6a). However, with total lifetime fuel cost as a primary driver, specific protocols will need to be developed to understand how MEA efficiency changes over the projected 1M mile lifetime of operation as performance assessments at BOL and after ASTs will not be enough to correctly project fuel cost for an MEA or system.

388 Drawing from a decade of LDV work focused on reducing overall Pt loading and improving
389 local oxygen transport,[7,78] **Figure 6a** illustrates how ionomer loading, Pt particle location and
390 accessibility,[61] ionomer adsorption,[79] ionomer conformation,[80] chemistry and confinement,[81] as
391 well as Pt/C/ionomer aggregation[82] offer opportunities to tailor electrocatalyst/ionomer
392 interactions and integration, resulting in improving overall electrode design for high-current-
393 density operation. The well-documented oxygen transport losses (R_{nF}), which occur near the
394 reaction site when operating low Pt roughness (*i.e.*, f_{Pt} [cm^2_{Pt} cm^{-2}_{MEA}] < 40) electrodes at high
395 current densities, have been shown to be the largest contributor to transport-related voltage loss
396 for LDV applications.[78,83] While 6b shows that the increased Pt content in HDV PEMFCs
397 significantly reduces these losses at BOL, local transport losses may continue to be a concern as
398 electrocatalyst surface area decreases at the end of stack life.

399 In PEMFC catalyst layers, ionomer is present across a distribution of nm-thick films on the
400 catalyst/support and as free aggregates (Figure 4). In the 5-50 nm film thickness regime, ionomer
401 behavior is influenced by confinement and substrate interactions, altering the film's structure and
402 limiting hydration and species mobility (*e.g.* reduced proton and O_2 transport).[74,79,84-92] The
403 variations in R_{nF} due to modifications of ionomer to carbon (I:C) ratio are related both to the
404 increasing proportion of thicker films[88,91,92] as well as increased ionomer aggregation resulting in
405 increased pore blocking in the bulk of the electrode and within the electrocatalyst aggregates.
406 While changes to ionomer equivalent weight (EW) have not been found to significantly affect
407 R_{nF} (**Figure 6a**), it has been found to affect the level of electrocatalyst agglomeration.
408 Consequently, modifications to ionomer chemistry/structure could further alter the ionomer-
409 catalyst interactions and local transport functionalities.[74,84,85,87-89,91,93]

410 Since the exact approaches and materials used to improve LDV performance may not be directly
411 translatable to HDVs, additional studies must be performed to begin to unlock the full potential
412 of high-performance materials within the electrode structure. In a recent example, a sulfonated
413 polymerized ionic liquid block copolymer was combined with Nafion and a Pt/Vu based
414 electrocatalyst to produce an MEA where Pt-oxide formation was suppressed at high potential,
415 enabling ORR specific activities on par with those obtained from ionomer-free (i.e., unpoisoned)
416 RDE experiments. As a result, the mixed ionomer electrode achieved a doubling of catalyst mass
417 activity.[94] While perhaps only pertinent to catalysts using non-porous supports where the vast
418 majority of electrocatalysts particles interact directly with the ionomer, there is an opportunity to
419 tailor the electrocatalyst/ionomer interface to enable higher efficiency HDV electrodes. Such
420 electrodes could further benefit from development of novel ionomers with high-gas permeation
421 and tunable substrate-interactions. Furthermore, despite an improved understanding across the
422 community, there is still a need to develop an ink-to-electrode structure understanding with
423 which one can dictate catalyst-layer structures by controlling catalyst/ionomer interactions in the
424 ink, utilizing optimized ink processing, and through tailored electrode break-in (conditioning)
425 procedures.

426
427 **Gas Diffusion Layers**
428
429 GDLs typically consist of a carbon black microporous layer (MPL) on top of carbonized fibers.
430 The whole layer is teflonated to form a mixed wettable material. These GDLs tend to show
431 decreasing hydrophobicity with operating time, which changes its ability to remove water,
432 thereby affecting performance. While these hydrophobicity changes have not been a primary

433 life-limiting factor for LDVs, the effects will be exacerbated with the longer HDV lifetime,
434 possibly requiring new materials or additional treatments. For example, the addition of
435 carboxymethyl-cellulose has been demonstrated to improve GDL durability when subjected to
436 both chemical and mechanical ASTs, dramatically reducing the change in power density, Ohmic
437 resistance, and mass-transport resistance.[95] Similarly, the use of microporous layers (MPLs) with
438 hydrophilic pores[96] and renewed investigations on the GDL/channel interface where droplet
439 shedding occurs demonstrate areas of increased interest for HDV PEMFC optimization.[97]
440
441 **Bipolar Plates**
442
443 Cost estimates indicate that bipolar plates represent approximately \$8.2/kW or 30% of the
444 PEMFC stack cost at production volumes of 500,000 systems per year.[98] Preferred materials, like
445 stainless steel or titanium, show inherent corrosion resistance such that imperfect corrosion-
446 resistant coatings do not result in significant release of corrosion products. However, as HDVs
447 require significantly longer lifetimes, small amounts of corrosion products such as Fe^{2+} may
448 prove problematic for membrane degradation as they act as Fenton's reagents to catalyze radical
449 formation. In addition, the cost of stainless steel (SS 316L) is estimated to be \$3.5/kW_{net}, which
450 is currently higher than the DOE target of \$3/kW for a complete plate,[98] thus less expensive
451 substrate materials are needed to meet commercialization targets. Titanium is an even more
452 expensive base material than stainless steel. A strong candidate is aluminum due to its low cost
453 and weight. Emphasis should be placed on developing cost-effective coatings for aluminum that
454 are defect-free, conductive, and corrosion resistant. Carbon-composite bipolar plates provide
455 another path forward to replace stainless steel; efforts should focus on improving their
456 volumetric power density.[99]

457 **Current status of commercial MEAs**

458 The current state-of-the-art (SOA) materials used in commercial LDVs can effectively serve as
459 the starting point and benchmark for the next-generation HDV components. The United States
460 Council for Automotive Research (USCAR) provided the Fuel Cell Performance and Durability
461 (FC-PAD) consortium with components from the Toyota Mirai FCEV, following 300hr of real-
462 world driving.[14,56] A small portion of this analysis is presented in **Figure 7.** Cross-sectional
463 views of the cell in **Figure 7a,b** show a 10μm-thick ionomer membrane reinforced with an
464 expanded hydrophobic polytetrafluoroethylene (ePTFE) layer for enhanced mechanical stability.
465 The electrodes are comprised of Pt (anode) and Pt-Co alloy (cathode) nanoparticle catalysts
466 supported on high surface area carbon, with a total Pt loading of approximately 0.4 mg_{Pt}/cm^2
467 (**Figure 7c**), similar to loadings expected for HDV applications. The mean particle size of the
468 $Pt_{0.92}Co_{0.08}$ cathode catalyst was 4.7 nm (**Figure 7f-g**), with the low Co loading reinforcing the
469 emphasis on durability over BOL performance. Despite the low loading, Co was found in the
470 membrane, supporting the earlier discussion regarding the need for dissolution-resistant
471 catalysts.
472
473 A non-homogeneous ionomer distribution within the cathode, with larger ionomer aggregates
474 near the membrane (shown in green) and regions of dense agglomerates (shown in red) that
475 exhibit limited ionomer infiltration (**Figure 7d**) illustrate the need for further electrode
476 optimization. Large ceria particles were added to the MPLs of the GDL for membrane
477 degradation mitigation. The bipolar plates (not pictured) were carbon-coated titanium with a 3-D
478 fine mesh flow field on the cathode. These observations from commercial LDVs demonstrate

479 that while much progress has been made, significant research and development is required to
480 meet not only LDV targets, but the enhanced durability and efficiency requirements for HDVs.
481 There remains a critical need to develop robust, efficient, and cost-effective MEAs tailored to the
482 HDV application with more emphasis on efficiency and durability rather than the cost of
483 components.
484

Outlook

485 **Outlook**

486 It is an exciting time for hydrogen and fuel cells. The rapid developments in fuel-cell materials,
487 integration, and manufacturing over the last decade will continue to accelerate as world-wide
488 interest in hydrogen grows as both a value proposition and means for decarbonizing our energy
489 system. In the transportation sector, we see an imminent shift in focus from light- to heavy-duty
490 applications. This shift is due in part to the decrease in Li-ion battery costs that are making
491 battery electric vehicles the incumbent technology for LDVs, as well as infrastructure challenges
492 with distributed hydrogen. While fuel cells remain advantageous compared to batteries in many
493 areas (*e.g.*, cost for increased driving range, refueling time, etc.) and will remain so with further
494 improvements, such differences greatly increase as one moves towards the heavy-duty and fleet
495 applications. Such a movement also ameliorates the hydrogen infrastructure challenges by
496 concentrating refueling stations.
497

498 However, even with this focus, early electrified HDVs will likely be battery driven due to
499 existing recharging infrastructure and earlier deployments. As fuel cell technology evolves, the
500 inherent advantages will provide for its rapid adoption, especially for high power applications
501 such as long-haul trucks, trains, buses, and maritime. The change in focus from light to heavy
502 duty vehicles exacerbates durability and efficiency challenges for fuel cells, necessitating
503 material and system innovations that enable new classes of hydrogen vehicles that take
504 advantage of the high efficiency, power density, and scalability of this technology. As HDVs
505 make their way to the road, installation of the required hydrogen infrastructure, in addition to the
506 increased levels of hydrogen production, distribution, use, and storage through the DOE
507 H2@Scale initiative, will pave the way for widespread adoption of light-duty FCEVs.
508

523 **Competing Interests**

524   The authors declare no competing interests

References

1   *The Future of Hydrogen* (International Energy Agency, 2019); https://www.iea.org/reports/the-future-of-hydrogen **Extensive study prepared for the G20 in Japan on the status of hydrogen in the global energy system and key near-term opportunities for rapidly expanding hydrogen use.**

2   *Road Map to a US Hydrogen Economy* (Fuel Cell & Hydrogen Energy Association, 2019); http://www.fchea.org/us-hydrogen-study

3   *Hydrogen Economy Outlook* (BloombergNEF, 2020); https://data.bloomberglp.com/professional/sites/24/BNEF-Hydrogen-Economy-Outlook-Key-Messages-30-Mar-2020.pdf

4   *Hydrogen Roadmap Europe* (Fuel Cells and Hydrogen Joint Undertaking, 2019); https://www.fch.europa.eu/

5   Carr, J. *Chinese Fuel Cell Industry Developments* (Fuel Cell & Hydrogen Energy Association Newsletter, 2019); http://www.fchea.org/in-transition/2019/2/4/chinese-fuel-cell-industry-developments

6   *The National Hydrogen Strategy* (Federal Ministry for Economic Affairs and Energy, 2020); https://www.bmbf.de/files/bmwi_Nationale%20Wasserstoffstrategie_Eng_s01.pdf

7   *Fuel Cell Technologies Office Multi-Year Research, Development, and Demonstration Plan* (US Department of Energy, 2013); https://www.energy.gov/eere/fuelcells/downloads/fuel-cell-technologies-office-multi-year-research-development-and-22

8   *H2@Scale* (US Department of Energy, 2017); https://www.energy.gov/eere/fuelcells/h2scale

9   Satyapal, S. *Hydrogen and Fuel Cell Program Overview* (Hydrogen & Fuel Cells Program Annual Merit Review Proceedings, 2019); https://www.hydrogen.energy.gov/pdfs/review19/plenary_overview_satyapal_2019.pdf

10   Luth, M. *Fuel Cell Customers - Medium and Heavy-Duty Transportation* (2019); http://www.fchea.org/in-transition/2019/9/2/fuel-cell-customers-medium-and-heavy-duty-transportation

11   *Average Annual Vehicle Miles Traveled by Major Vehicle Category* (EERE Alternative Fuels Data Center, 2020); https://afdc.energy.gov/data/

12   *Vehicle Miles Traveled by Highway Category and Vehicle Type* (Bureau of Transportation Statistics, 2018); https://www.bts.gov/vehicle-miles-traveled-highway-category-and-vehicle-type

13   Davis, S.C., Williams, S.E. & Boundy, R.G. *Transportation Energy Data Book: Edition 36*. (2017).

14   *Fast Facts on Transportation Greenhouse Gas Emissions* (United States Environmental Protection Agency, 2017); https://www.epa.gov/greenvehicles/fast-facts-transportation-greenhouse-gas-emissions

15   *Annual Energy Outlook 2019* (U.S. Energy Information Administration, 2019); https://www.eia.gov/outlooks/aeo/pdf/aeo2019.pdf

16   Ding, Y., Cano, Z.P., Yu, A., Lu, J. & Chen, Z. Automotive Li-Ion batteries: Current status and future perspectives. *Electrochem. Energy Rev.* **2**, 1-28, doi:10.1007/s41918-018-0022-z (2019).

17   Lutsey, N. & Nicholas, M. *Update on electric vehicle costs in the United States through 2030* (2019); https://theicct.org/sites/default/files/publications/EV_cost_2020_2030_20190401.pdf

18   *Early Markets: Fuel Cells for Material Handling Equipment* (US Department of Energy, 2016); https://www.energy.gov/sites/prod/files/2016/12/f34/fcto_early_markets_mhe_fact_sheet.pdf

19   Guandalini, G. in *2018 International Conference of Electrical and Electronic Technologies for Automotive* (2018).

20 Eudy, L. *Fuel Cell Buses in U.S. Transit Fleets: Current Status 2018* (2018); https://www.nrel.gov/docs/fy19osti/72208.pdf

21 Lozanovski, A., Whitehouse, N., Ko, N. & Whitehouse, S. Sustainability assessment of fuel cell buses in public transport. *Sustainability* **10**, 1480, doi:10.3390/su10051480 (2018).

22 Ahluwalia, R.K. *et al. Total Cost of Ownership for Line Haul, Yard Switchers and Regional Passenger Locomotives − Preliminary Results* (H2@Ports Workshop, H2@Ports Workshop, 2019); https://www.energy.gov/eere/fuelcells/h2rail-workshop

23 Papadias, D., Ahluwalia, R.K., Connelly, E. & Devlin, P. *Total Cost of Ownership Analysis for Hydrogen Fuel Cells in Maritime Applications: Preliminary Results* (H2@Ports Workshop, 2019); https://www.energy.gov/eere/fuelcells/h2ports-workshop

24 Marcinkoski, J. *et al. Hydrogen Class 8 Long Haul Truck Targets* (2019); https://www.hydrogen.energy.gov/pdfs/19006_hydrogen_class8_long_haul_truck_targets.pdf **Identifies critical technical targets for reducing the cost of ownership of hydrogen fuel cell powered Class 8 tractor-trailers to be to be competitive with diesel-powered vehicles.**

25 Johansson, K. *The Effect of Drive Cycles on the Performance of a PEM Fuel Cell System for Automotive Applications* (2001); https://www.sae.org/publications/technical-papers/content/2001-01-3454/

26 *Dynamometer Drive Schedules* (United States Environmental Protection Agency, 2019); https://www.epa.gov/vehicle-and-fuel-emissions-testing/dynamometer-drive-schedules

27 *Greenhouse Gas Emissions and Fuel Efficiency Standards for Medium- and Heavy-Duty Engines and Vehicles—Phase 2* (Environmental Protection Agency, 2016); https://www.govinfo.gov/content/pkg/FR-2016-10-25/pdf/2016-21203.pdf

28 Franco, V., Delgado, O. & Muncrief, R. *Heavy-Duty Vehicle Fuel-Efficiency Simulation: A Comparison of US and EU Tools* (International Council on Clean Transportation, 2015); https://theicct.org/sites/default/files/publications/ICCT_GEM-VECTO-comparison_20150511.pdf

29 Ahluwalia, R.K., Wang, X. & Peng, J.-K. *Fuel Cell System Modeling and Analysis* (Hydrogen & Fuel Cells Program Annual Merit Review Proceedings, 2020); https://www.hydrogen.energy.gov/pdfs/review20/fc017_ahluwalia_2020_o.pdf

30 Yu, Y. *et al.* A review on performance degradation of proton exchange membrane fuel cells during startup and shutdown processes: Causes, consequences, and mitigation strategies. *J. Power Sources* **205**, 10-23, doi:https://doi.org/10.1016/j.jpowsour.2012.01.059 (2012).

31 Zhang, T., Wang, P., Chen, H. & Pei, P. A review of automotive proton exchange membrane fuel cell degradation under start-stop operating condition. *App. Energy* **223**, 249-262, doi:10.1016/j.apenergy.2018.04.049 (2018). **A comprehensive review of degradation mechanisms, accelerated lifetime tests and mitigation strategies for PEMFC start-up/shut-down.**

32 Reiser, C.A. *et al.* A reverse-current decay mechanism for fuel cells. *Electrochem. Solid-State Lett.* **8**, A273, doi:10.1149/1.1896466 (2005).

33 Kojima, T.Y.a.K. Toyota MIRAI fuel cell vehicle and progress toward a future hydrogen society. *Electrochem. Soc. Interface* **24**, 45-49, doi:10.1149/2.F03152if (2015).

34 Gittleman, C.S., Kongkanand, A., Masten, D. & Gu, W. Materials research and development focus areas for low cost automotive proton-exchange membrane fuel cells. *Curr. Opin. Electrochem.* **18**, 81-89, doi:10.1016/j.coelec.2019.10.009 (2019).

35 Wan, Z., Chang, H., Shu, S., Wang, Y. & Tang, H. A review on cold start of proton exchange membrane fuel cells. *Energies* **7**, 3179-3203, doi:10.3390/en7053179 (2014).

618   36   Amamou, A.A., Kelouwani, S., Boulon, L. & Agbossou, K. A comprehensive review of solutions
619   and strategies for cold start of automotive proton exchange membrane fuel cells. *IEEE Access* **4**,
620   4989-5002, doi:10.1109/access.2016.2597058 (2016).

621   37   Cheng, X. *et al.* A review of PEM hydrogen fuel cell contamination: Impacts, mechanisms, and
622   mitigation. *J. Power Sources* **165**, 739-756, doi:10.1016/j.jpowsour.2006.12.012 (2007).

623   38   Wang, X.X., Swihart, M.T. & Wu, G. Achievements, challenges and perspectives on cathode
624   catalysts in proton exchange membrane fuel cells for transportation. *Nat. Catal.* **2**, 578-589,
625   doi:10.1038/s41929-019-0304-9 (2019). **Comprehensive review of state-of-the-art oxygen**
626   **reduction reaction electrocatalysts and high surface area carbon supports for proton exchange**
627   **membrane fuel cells.**

628   39   Chung, D.Y., Yoo, J.M. & Sung, Y.E. Highly Durable and Active Pt-Based Nanoscale Design for
629   Fuel-Cell Oxygen-Reduction Electrocatalysts. *Advanced Materials* **30**, e1704123,
630   doi:10.1002/adma.201704123 (2018).

631   40   Banham, D. & Ye, S. Current status and future development of catalyst materials and catalyst
632   layers for proton exchange membrane fuel cells: An industrial perspective. *ACS Energy Lett.* **2**,
633   629-638, doi:10.1021/acsenergylett.6b00644 (2017).

634   41   Thompson, S.T. & Papageorgopoulos, D. Platinum group metal-free catalysts boost cost
635   competitiveness of fuel cell vehicles. *Nat. Catal.* **2**, 558-561, doi:10.1038/s41929-019-0291-x
636   (2019).

637   42   Sneed, B.T., Cullen, D.A., Mukundan, R., Borup, R.L. & More, K.L. PtCo cathode catalyst
638   morphological and compositional changes after PEM fuel cell accelerated stress testing. *J.*
639   *Electrochem. Soc.* **165**, F3078-F3084, doi:10.1149/2.0091806jes (2018).

640   43   Papadias, D.D. *et al.* Durability of Pt-Co alloy polymer electrolyte fuel cell cathode catalysts
641   under accelerated stress tests. *J. Electrochem. Soc.* **165**, F3166-F3177, doi:10.1149/2.0171806jes
642   (2018).

643   44   Ioroi, T., Siroma, Z., Yamazaki, S.i. & Yasuda, K. Electrocatalysts for PEM fuel cells. *Adv. Energy*
644   *Mat.* **9**, 1801284, doi:10.1002/aenm.201801284 (2018).

645   45   Yang, Z., Ball, S., Condit, D. & Gummalla, M. Systematic study on the impact of Pt particle size
646   and operating conditions on PEMFC cathode catalyst durability. *J. Electrochem. Soc.* **158**, B1439,
647   doi:10.1149/2.081111jes (2011).

648   46   Gummalla, M. *et al.* Effect of particle size and operating conditions on Pt3Co PEMFC cathode
649   catalyst durability. *Catalysts* **5**, 926-948, doi:10.3390/catal5020926 (2015).

650   47   Yasuda, K., Taniguchi, A., Akita, T., Ioroi, T. & Siroma, Z. Platinum dissolution and deposition in
651   the polymer electrolyte membrane of a PEM fuel cell as studied by potential cycling. *Physical*
652   *Chemistry Chemical Physics* **8**, 746-752, doi:10.1039/b514342j (2006).

653   48   Ahluwalia, R.K. *et al.* Potential dependence of Pt and Co dissolution from platinum-cobalt alloy
654   PEFC catalysts using time-resolved measurements. *J. Electrochem. Soc.* **165**, F3024-F3035,
655   doi:10.1149/2.0031806jes (2018).

656   49   Shao-Horn, Y. *et al.* Instability of supported platinum nanoparticles in low-temperature fuel
657   cells. *Top. Catal.* **46**, 285-305, doi:10.1007/s11244-007-9000-0 (2007).

658   50   de Bruijn, F.A., Dam, V.A.T. & Janssen, G.J.M. Review: Durability and degradation issues of PEM
659   fuel cell components. *Fuel Cells* **8**, 3-22, doi:10.1002/fuce.200700053 (2008).

660   51   Meier, J.C. *et al.* Design criteria for stable Pt/C fuel cell catalysts. *Beilstein J. Nanotechnol.* **5**, 44-
661   67, doi:10.3762/bjnano.5.5 (2014).

662   52   Cherevko, S., Kulyk, N. & Mayrhofer, K.J.J. Durability of platinum-based fuel cell electrocatalysts:
663   Dissolution of bulk and nanoscale platinum. *Nano Energy* **29**, 275-298,
664   doi:10.1016/j.nanoen.2016.03.005 (2016).

665   53   Watanabe, M., Yano, H., Uchida, H. & Tryk, D.A. Achievement of distinctively high durability at
666   nanosized Pt catalysts supported on carbon black for fuel cell cathodes. *J. Electroanal. Chem.*
667   **819**, 359-364, doi:10.1016/j.jelechem.2017.11.017 (2018).
668   54   Xin, H.L. *et al.* Atomic-resolution spectroscopic imaging of ensembles of nanocatalyst particles
669   across the life of a fuel cell. *Nano Lett.* **12**, 490-497, doi:10.1021/nl203975u (2012).
670   55   Lohse-Busch, H. *et al. Technology Assessment of a Fuel Cell Vehicle: 2017 Toyota Mirai* (Argonne
671   National Laboratory, 2018);
672   56   Borup, R.L. *et al.* Recent developments in catalyst-related PEM fuel cell durability. *Curr. Opin.*
673   *Electrochem.* **21**, 192-200, doi:10.1016/j.coelec.2020.02.007 (2020).
674   57   Braaten, J., Kongkanand, A. & Litster, S. Oxygen transport effects of cobalt cation contamination
675   of ionomer thin films in proton exchange membrane fuel cells. *ECS Trans.* **80** 283-290 (2017).
676   58   Li, J. *et al.* Hard-magnet L10-CoPt nanoparticles advance fuel cell catalysis. *Joule* **3**, 124-135,
677   doi:10.1016/j.joule.2018.09.016 (2019).
678   59   Yin Xiong, Y.Y., Howie Joress, Elliot Padgett, Unmukt Gupta, Venkata Yarlagadda,, David N.
679   Agyeman-Budu, X.H., Thomas E. Moylan, Rui Zeng, Anusorn Kongkanand, Fernando A. Escobedo,
680   & Joel D. Brock, F.J.D., David A. Muller, and Héctor D. Abruña. Revealing the atomic ordering of
681   binary intermetallics using in situ heating techniques at multilength scales. *PNAS* **116**, 1974–
682   1983, doi:doi/10.1073/pnas.1815643116 (2019).
683   60   Padgett, E. *et al.* Mitigation of PEM fuel cell catalyst degradation with porous carbon supports. *J.*
684   *Electrochem. Soc.* **166**, F198-F207, doi:10.1149/2.0371904jes (2019). **Investigation on the**
685   **impact of carbon support morphology, ranging from porous to solid, on the performance and**
686   **durability of Pt and PtCo alloy nanoparticle cathode electrocatalysts.**
687   61   Yarlagadda, V. *et al.* Boosting Fuel Cell Performance with Accessible Carbon Mesopores. *ACS*
688   *Energy Lett.* **3**, 618-621, doi:10.1021/acsenergylett.8b00186 (2018).
689   62   Wang, Y.J., Wilkinson, D.P. & Zhang, J. Noncarbon support materials for polymer electrolyte
690   membrane fuel cell electrocatalysts. *Chem. Rev.* **111**, 7625-7651, doi:10.1021/cr100060r (2011).
691   63   Sui, S. *et al.* A comprehensive review of Pt electrocatalysts for the oxygen reduction reaction:
692   Nanostructure, activity, mechanism and carbon support in PEM fuel cells. *J. Mater. Chem. A* **5**,
693   1808-1825, doi:10.1039/c6ta08580f (2017).
694   64   Qiao, Z. *et al.* 3D porous graphitic nanocarbon for enhancing the performance and durability of
695   Pt catalysts: a balance between graphitization and hierarchical porosity. *Energy Environ. Sci.* **12**,
696   2830-2841, doi:10.1039/c9ee01899a (2019).
697   65   Cheng, N. *et al.* Extremely stable platinum nanoparticles encapsulated in a zirconia nanocage by
698   area-selective atomic layer deposition for the oxygen reduction reaction. *Adv. Mater.* **27**, 277-
699   281, doi:10.1002/adma.201404314 (2015).
700   66   Chen, Y. *et al.* Pt–SnO2/nitrogen-doped CNT hybrid catalysts for proton-exchange membrane
701   fuel cells (PEMFC): Effects of crystalline and amorphous SnO2 by atomic layer deposition. *J.*
702   *Power Sources* **238**, 144-149, doi:10.1016/j.jpowsour.2013.03.093 (2013).
703   67   Yamada, H., Kato, H. & Kodama, K. Cell performance and durability of Pt/C cathode catalyst
704   covered by dopamine derived carbon thin layer for polymer electrolyte fuel cells. *J. Electrochem.*
705   *Soc.* **167**, 084508, doi:10.1149/1945-7111/ab8b97 (2020).
706   68   T. J. Schmidt, H.A.G., G. D. Stab, P. M. Urban, D. M. Kolb, and R. J. Behm. Characterization of
707   high-surface-area electrocatalysts using a rotating disk electrode configuration. *J. Electrochem.*
708   *Soc.* **145**, 2354-2358 (1998).
709   69   Gilbert, J.A. *et al.* In-operando anomalous small-angle X-Ray scattering investigation of Pt3Co
710   catalyst degradation in aqueous and fuel cell environments. *J. Electrochem. Soc.* **162**, F1487-
711   F1497, doi:10.1149/2.0531514jes (2015).

17

712 70   Tian, N. *et al.* Rational design and synthesis of low-temperature fuel cell clectrocatalysts.
713   *Electrochem. Energy Rev.* **1**, 54-83, doi:10.1007/s41918-018-0004-1 (2018).
714 71   Gubler, L., Nauser, T., Coms, F.D., Lai, Y.-H. & Gittleman, C.S. Perspective—Prospects for durable
715   hydrocarbon-based fuel cell membranes. *J. Electrochem. Soc.* **165**, F3100-F3103,
716   doi:10.1149/2.0131806jes (2018). **Perspective on critical breakthroughs required to replace**
717   **PFSA with hydrocarbon-based membranes that are currently limited by radical-induced**
718   **degradation and mechanical failure.**
719 72   Elabd, Y.A. & Hickner, M.A. Block copolymers for fuel cells. *Macromolecules* **44**, 1-11,
720   doi:10.1021/ma101247c (2011).
721 73   Kusoglu, A. & Weber, A.Z. New insights into perfluorinated sulfonic-acid ionomers. *Chem. Rev.*
722   **117**, 987-1104, doi:10.1021/acs.chemrev.6b00159 (2017).
723 74   Kusoglu, A., Dursch, T.J & Weber, A.Z. Nanostructure/swelling relationships of bulk and thin-film
724   PFSA ionomers. *Adv. Funct. Mater.* **26**, 4961-4975, doi:10.1002/adfm.201600861 (2016).
725 75   Yandrasits, M., Lindell, M., Schaberg, M. & Kurkowski, M. Increasing fuel cell efficiency by using
726   ultra-low equivalent weight ionomers. *Electrochem. Soc. Interface* **26**, 49-53 (2017). **Discusses**
727   **the material design paths toward lower equivalent-weight ionomers via side-chain chemistry**
728   **modifications to enable higher conductivity at low humidity for increased fuel-cell efficiency.**
729 76   Su, G.M. *et al.* Chemical and morphological origins of improved ion conductivity in perfluoro
730   ionene chain extended ionomers. *J. Am. Chem. Soc.* **141**, 13547-13561,
731   doi:10.1021/jacs.9b05322 (2019).
732 77   E. L. Redmond, S.M.W., and J. L. Szarka III. Full factorial experiment to determine and predict
733   impact of cerium amount on fuel cell performance. *ECS Transactions* **80**, 633-641 (2017).
734 78   Kongkanand, A. & Mathias, M.F. The priority and challenge of high-power performance of low-
735   platinum proton-exchange membrane fuel cells. *J. Phys. Chem. Lett.* **7**, 1127-1137,
736   doi:10.1021/acs.jpclett.6b00216 (2016).
737 79   Kudo, K., Jinnouchi, R. & Morimoto, Y. Humidity and temperature dependences of oxygen
738   transport resistance of nafion thin film on platinum electrode. *Electrochim. Acta* **209**, 682-690,
739   doi:10.1016/j.electacta.2016.04.023 (2016).
740 80   Van Cleve, T. *et al.* Dictating Pt-based electrocatalyst performance in polymer electrolyte fuel
741   cells; from formulation to application. *ACS Appl. Mater. Inter.*, doi:10.1021/acsami.9b17614
742   (2019).
743 81   Eastman, S.A. *et al.* Effect of confinement on structure, water solubility, and water transport in
744   nafion thin films. *Macromolecules* **45**, 7920-7930, doi:10.1021/ma301289v (2012).
745 82   Cetinbas, F.C., Ahluwalia, R.K., Kariuki, N.N., De Andrade, V. & Myers, D.J. Effects of porous
746   carbon morphology, agglomerate structure and relative humidity on local oxygen transport
747   resistance. *J. Electrochem. Soc.* **167**, 013508, doi:10.1149/2.0082001jes (2019).
748 83   Weber, A.Z. & Kusoglu, A. Unexplained transport resistances for low-loaded fuel-cell catalyst
749   layers. *J. Mater. Chem. A* **2**, 17207-17211, doi:10.1039/c4ta02952f (2014).
750 84   Kodama, K. *et al.* Effect of the side-chain structure of perfluoro-sulfonic acid ionomers on the
751   oxygen reduction reaction on the surface of Pt. *ACS Catal.* **8**, 694-700,
752   doi:10.1021/acscatal.7b03571 (2018).
753 85   Nagao, Y. Proton-conductivity enhancement in polymer thin films. *Langmuir* **33**, 12547-12558,
754   doi:10.1021/acs.langmuir.7b01484 (2017).
755 86   Jinnouchi, R., Kudo, K., Kitano, N. & Morimoto, Y. Molecular dynamics simulations on O-2
756   permeation through nafion ionomer on platinum surface. *Electrochim. Acta* **188**, 767-776,
757   doi:10.1016/j.electacta.2015.12.031 (2016).

758 87 Ono, Y., Ohma, A., Shinohara, K. & Fushinobu, K. Influence of equivalent weight of ionomer on
759 local oxygen transport resistance in cathode catalyst layers. *J. Electrochem. Soc.* **160**, F779-F787,
760 doi:10.1149/2.040308jes (2013).
761 88 Kusoglu, A. in *Encyclopedia of Sustainability Science and Technology* (ed Robert A. Meyers) Ch.
762 Chapter 1021-2, 1-23 (Springer New York, 2018).
763 89 Tesfaye, M., MacDonald, A.N., Dudenas, P.J., Kusoglu, A. & Weber, A.Z. Exploring
764 substrate/ionomer interaction under oxidizing and reducing environments. *Electrochem.*
765 *Commun.* **87**, 86-90, doi:10.1016/j.elecom.2018.01.004 (2018).
766 90 Kusoglu, A. *et al.* Impact of substrate and processing on confinement of nafion thin films. *Adv.*
767 *Funct. Mater.* **24**, 4763-4774, doi:10.1002/adfm.201304311 (2014).
768 91 Ohma, A. *et al.* Analysis of proton exchange membrane fuel cell catalyst layers for reduction of
769 platinum loading at Nissan. *Electrochim. Acta* **56**, 10832-10841 (2011).
770 92 Cetinbas, F.C. *et al.* Hybrid approach combining multiple characterization techniques and
771 simulations for microstructural analysis of proton exchange membrane fuel cell electrodes. *J.*
772 *Power Sources* **344**, 62-73, doi:10.1016/j.jpowsour.2017.01.104 (2017).
773 93 Chen, Y. *et al.* Electrochemical study of temperature and Nafion effects on interface property for
774 oxygen reduction reaction. *Ionics* **24**, 3905-3914, doi:10.1007/s11581-018-2533-3 (2018).
775 94 Li, Y. *et al.* Modifying the electrocatalyst-ionomer interface via sulfonated poly(ionic liquid) block
776 copolymers to enable high-performance polymer electrolyte fuel cells. *ACS Energy Lett.* **5**, 1726–
777 1731 (2020). **Achieved ionomer-free Pt specific activity in an MEA, thereby enhancing**
778 **performance across a range of relative humidity using novel ionomers and a mixed ionomer**
779 **electrode.**
780 95 S. Latorrata. Gallo Stampino, E.A., R.Pelosato, C.Cristiani, G.Dotelli. Effect of rheology controller
781 agent addition to Micro-Porous Layers on PEMFC performances. *Solid State Ionics* **216**, 73-77.
782 96 Spernjak, D. *et al.* Enhanced water management of polymer electrolyte fuel cells with additive-
783 containing microporous layers. *ACS Appl. Energy Mater.* **1**, 6006-6017,
784 doi:10.1021/acsaem.8b01059 (2018).
785 97 Steinbach, A.J. *et al.* Anode-design strategies for improved performance of polymer-electrolyte
786 fuel cells with ultra-thin electrodes. *Joule* **2**, 1297-1312, doi:10.1016/j.joule.2018.03.022 (2018).
787 98 James, B. *Fuel Cell Vehicle and Bus Cost Analysis* (2016);
788 https://www.hydrogen.energy.gov/pdfs/review16/fc018_james_2016_o.pdf
789 99 James, B. *Fuel Cell Systems Analysis* (Hydrogen & Fuel Cells Program Annual Merit Review
790 Proceedings, 2020);
791 https://www.hydrogen.energy.gov/pdfs/review20/fc163_james_2020_o.pdf
792 100 *How hydrogen empowers the energy transition* (Hydrogen Council, 2017);
793 https://hydrogencouncil.com/wp-content/uploads/2017/06/Hydrogen-Council-Vision-
794 Document.pdf
795 101 US Department of Energy. *Fuel Cell Truck Powertrain R&D Activities and Target Review*
796 *Workshop* (2018); https://www.energy.gov/eere/fuelcells/fuel-cell-truck-powertrain-rd-
797 activities-and-target-review-workshop-h2-scale-end-use
798 102 Borup, R.L. & Weber, A.Z. *FC-PAD: Fuel Cell Performance and Durability Consortium* (Hydrogen &
799 Fuel Cells Program Annual Merit Review Proceedings, 2020);
800 https://www.hydrogen.energy.gov/pdfs/review20/fc135_borup_weber_2020_o.pdf
801 103 Van Cleve, T. *et al.* Tailoring electrode microstructure via ink content to enable improved rated
802 power performance for platinum cobalt/high surface area carbon based polymer electrolyte fuel
803 cells. *J. Power Sources* **482**, doi:10.1016/j.jpowsour.2020.228889 (2021).
804 104 Greszler, T.A., Caulk, D. & Sinha, P. The Impact of Platinum Loading on Oxygen Transport
805 Resistance. *J. Electrochem. Soc.* **159**, F831-F840, doi:10.1149/2.061212jes (2012).

806   105   Haug, A. *Novel ionomers and electrode structures for improved PEMFC electrode performance at*
807   *low PGM loadings* (Hydrogen & Fuel Cells Program Annual Merit Review Proceedings, 2019);
808   https://www.hydrogen.energy.gov/pdfs/review19/fc155_haug_2019_o.pdf
809   106   Borup, R.L. & Weber, A.Z. *FC-PAD: Fuel Cell Performance and Durability Consortium* (Hydrogen &
810   Fuel   Cells   Program   Annual   Merit   Review   Proceedings,   2019);
811   https://www.hydrogen.energy.gov/pdfs/review19/fc135_borup_2019_o.pdf
812   107   Borup, R.L., More, K.L. & Weber, A.Z. *FC-PAD: Fuel Cell Performance and Durability Consortium*
813   (Hydrogen   &   Fuel   Cells   Program   Annual   Merit   Review   Proceedings,   2018);
814   https://www.hydrogen.energy.gov/pdfs/review18/fc135_borup_2018_o.pdf
815
816

a **Hydrogen Fuel Cell Diversity in Transportation**
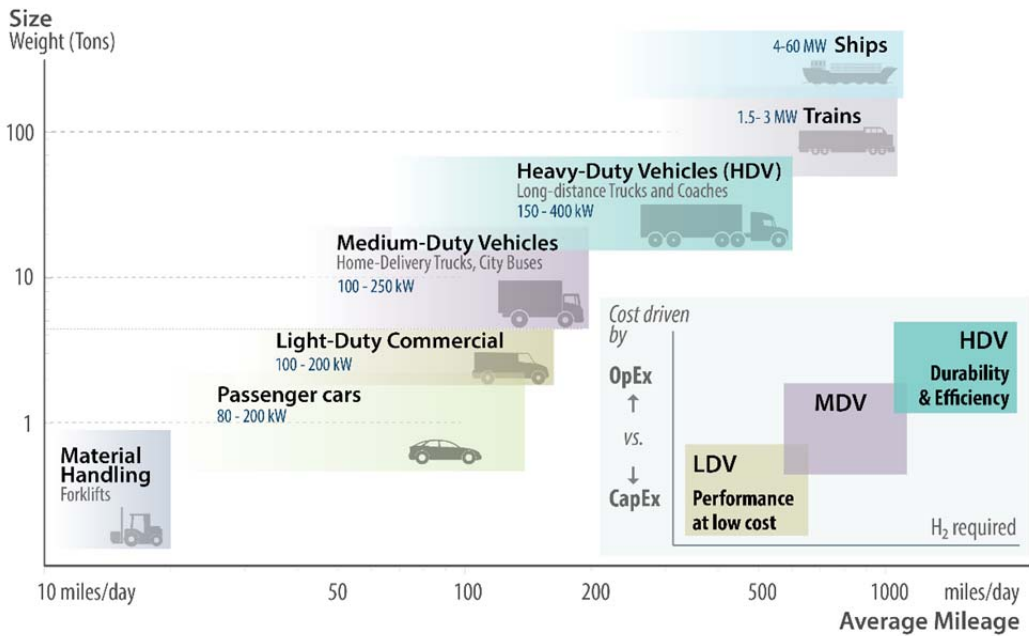
b Average Annual Vehicle Miles Traveled by Major Vehicle Category

c Potential Hydrogen demand market size

817
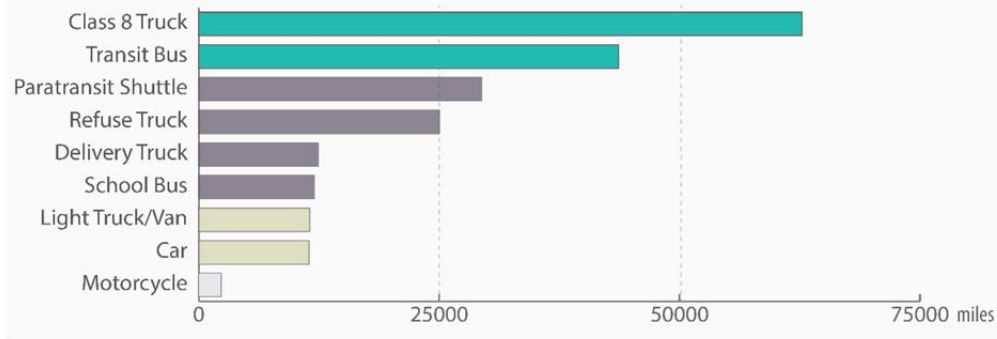
Figure 1. Roadmap to Hydrogen Fuel-Cells for Transportation. (a) Illustration of roadmap
for transition from light-duty and automotive fuel cells to medium- and heavy-duty applications
highlighting the paradigm shift in daily mileage and power output needs. The diagram is created
by compiling information from various reports.[4,19,100,101] The inset demonstrates the trade-off
between the OpEx and CapEx-driven costs for three classes of vehicles. **(b)** Annual miles
traveled per major vehicle category in the US.[11] **(c)** Projected hydrogen economy and market for
LDV and HDVs.[2]

21

825
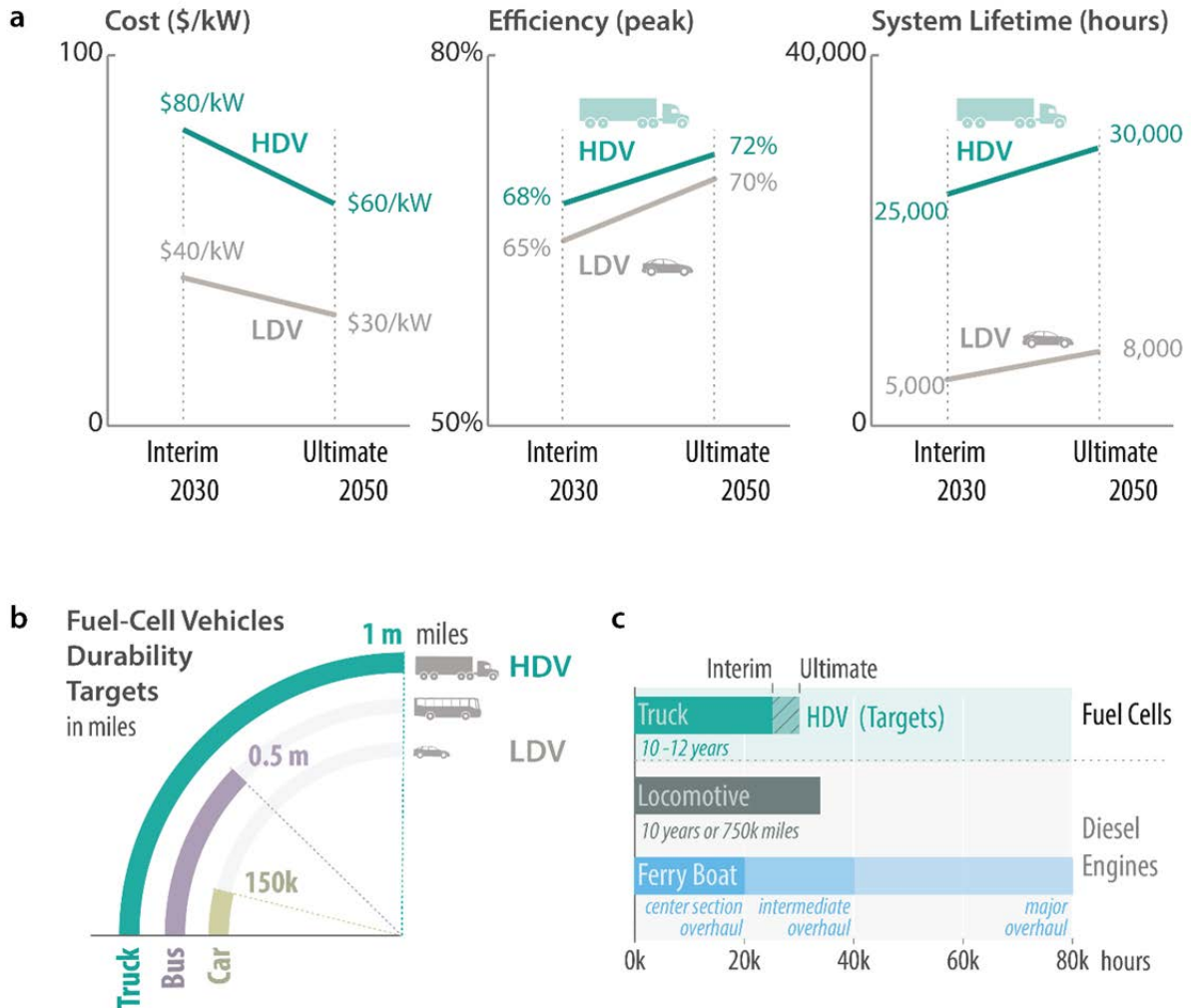
826
Figure 2. Summary of fuel cell targets and lifetimes. (a) Key interim and ultimate DOE fuel cell targets for automotive and trucks.[24] Current target of $50/kW for LDV is based on 100,000 units/year; HDV Targets are for Class 8 Tractor-Trailers. Ultimate targets are based on simple cost of ownership assumptions and reflects anticipated timeframe for market penetration. **(b)** Fuel cell durability targets for light- and heavy-duty vehicles expressed in terms of miles.[24] **(c)** Comparison of HDV fuel cell lifetime targets with the useful service lifetime of current diesel engines for rail (www.efrc.gov) and marine (www.wsdot.wa.gov/ferries/) applications.[22,23]

834

22
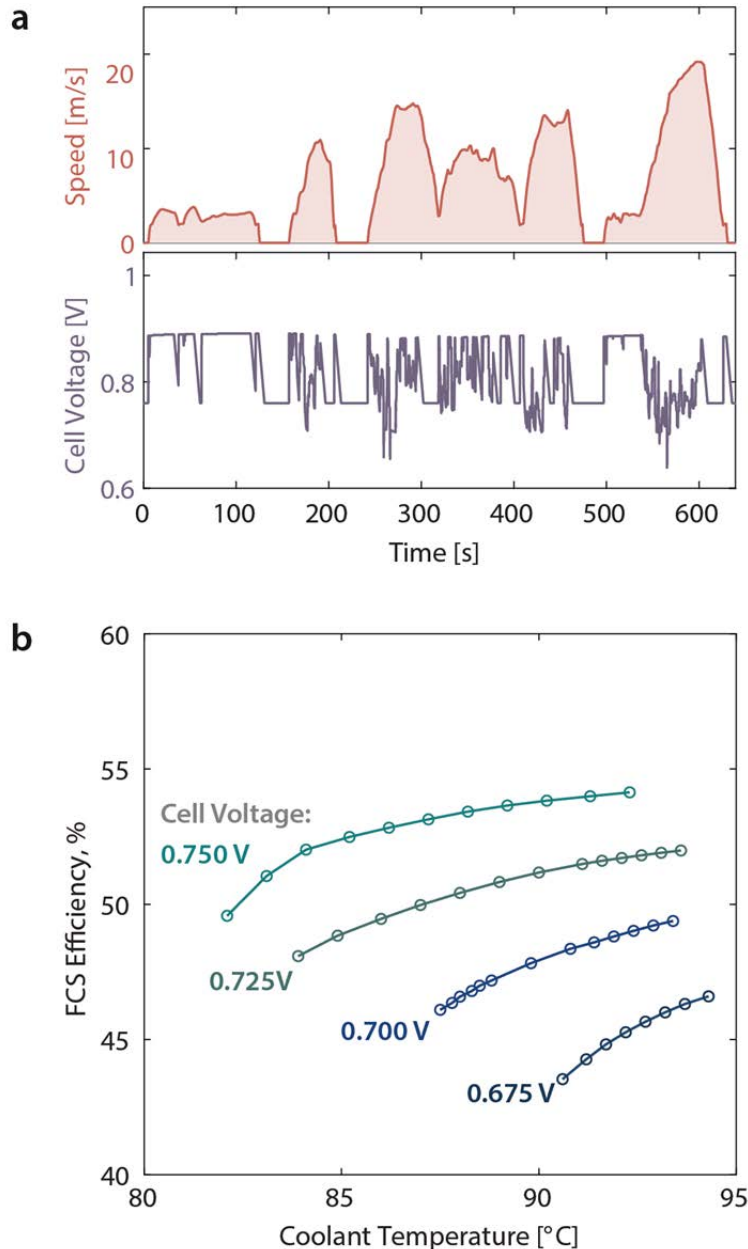
Figure 3. System demand and strategies for a HDV fuel cell system (FCS). (a) A representative HDV drive cycle for a Class 8 truck defined by the California Air Resource Board (ARB).[27] The cell voltages on this drive cycle were simulated for a hybrid 275kW FCS, 35kWh battery traction power system by assuming a minimum idle power of 20kW to limit the upper potential. **(b)** Relationship between the cell voltage at rated power and coolant temperature needed to reject waste heat at 6% grade.[29] Higher voltages allow operation at lower temperature and lead to higher efficiency but also lower power density (larger stack size). Panels adapted from pages 20 and 21 of ref.[29], 2020 DOE Annual Merit Review.

a Fuel Cell Components: "design space" for heavy duty stack with materials of the future
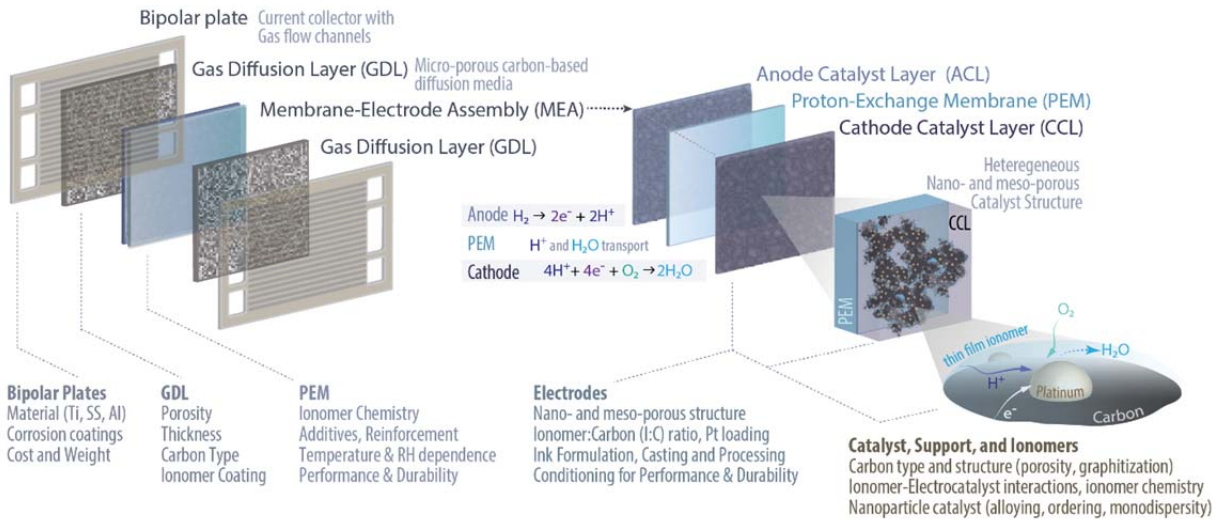
847
848 **Figure 4. Design space for fuel cells.** Components of a PEMFC stack with materials and design
849 parameters and close-up view of the MEA and cathode catalyst structure, shown with
850 anode/cathode reactions and illustration of heterogeneous porous structure of the catalyst layer
851 and the interactions between ionomer thin-film, carbon support and Pt catalyst particles.

852
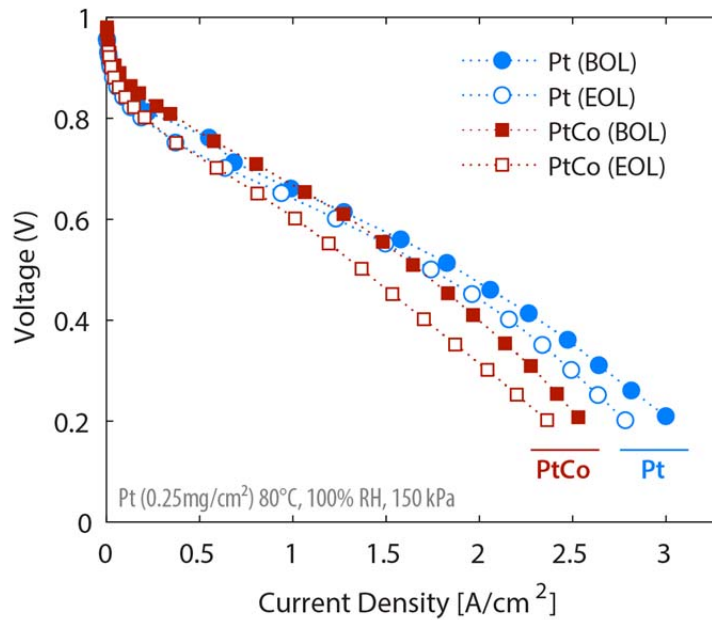
853

854 **Figure 5. Impact of catalyst alloying on fuel-cell performance change over lifetime.**
855 Polarization curves at BOL and after 75,000 cycles of the square wave AST, for a Pt/C (Blue
856 circles) and a PtCo/C (Red square) cathode catalyst-based MEA with a Pt loading of
857 0.25mg$_{Pt}$/cm^2. Reproduced from page 21 of ref.[102], 2020 DOE Annual Merit Review.

858

859
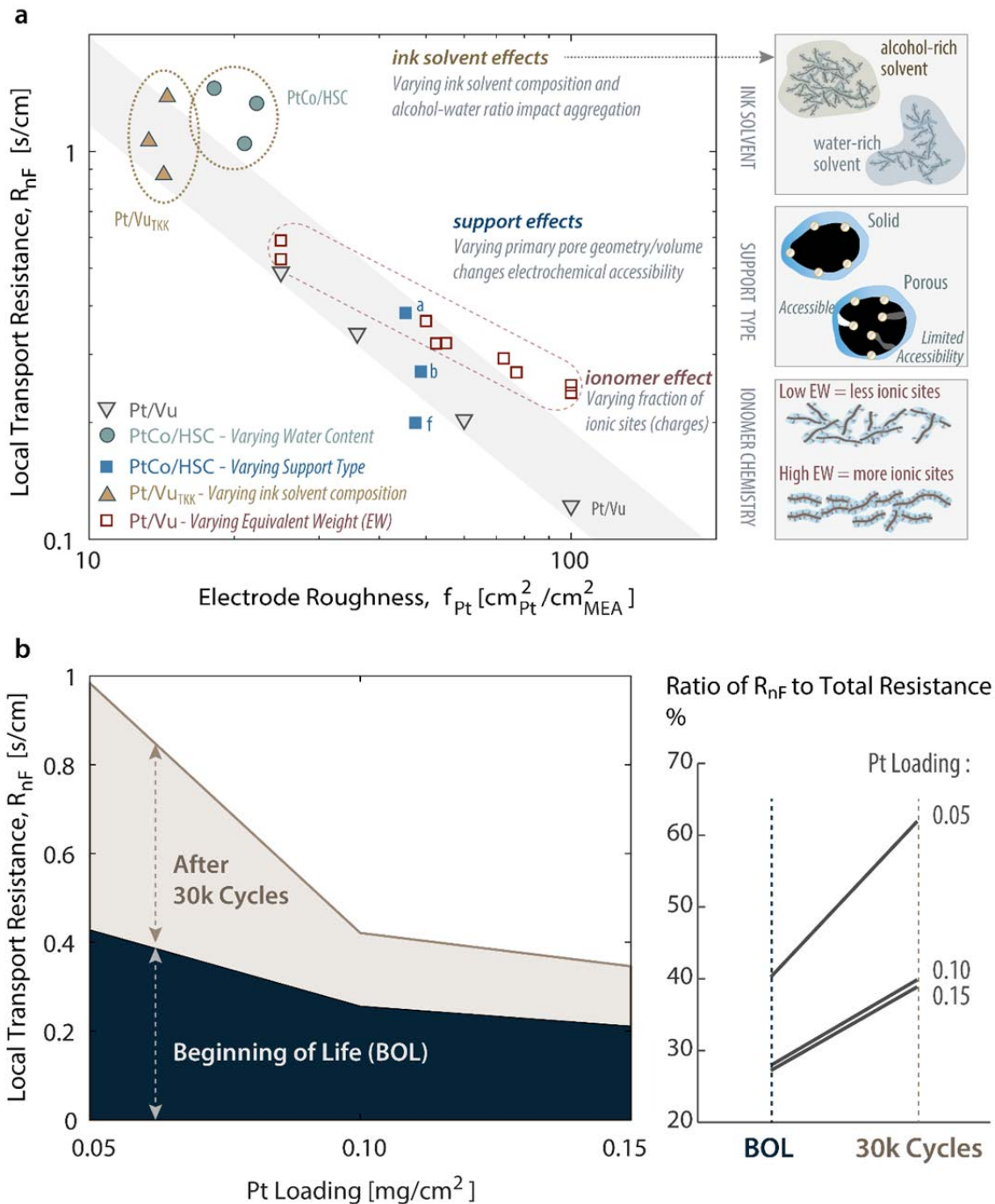
Figure 6. Performance-Durability impact on transport resistance in fuel cell electrodes. (a)
Cathode CL local transport resistance (non-Fickian oxygen transport resistance - R_{nF}) as a
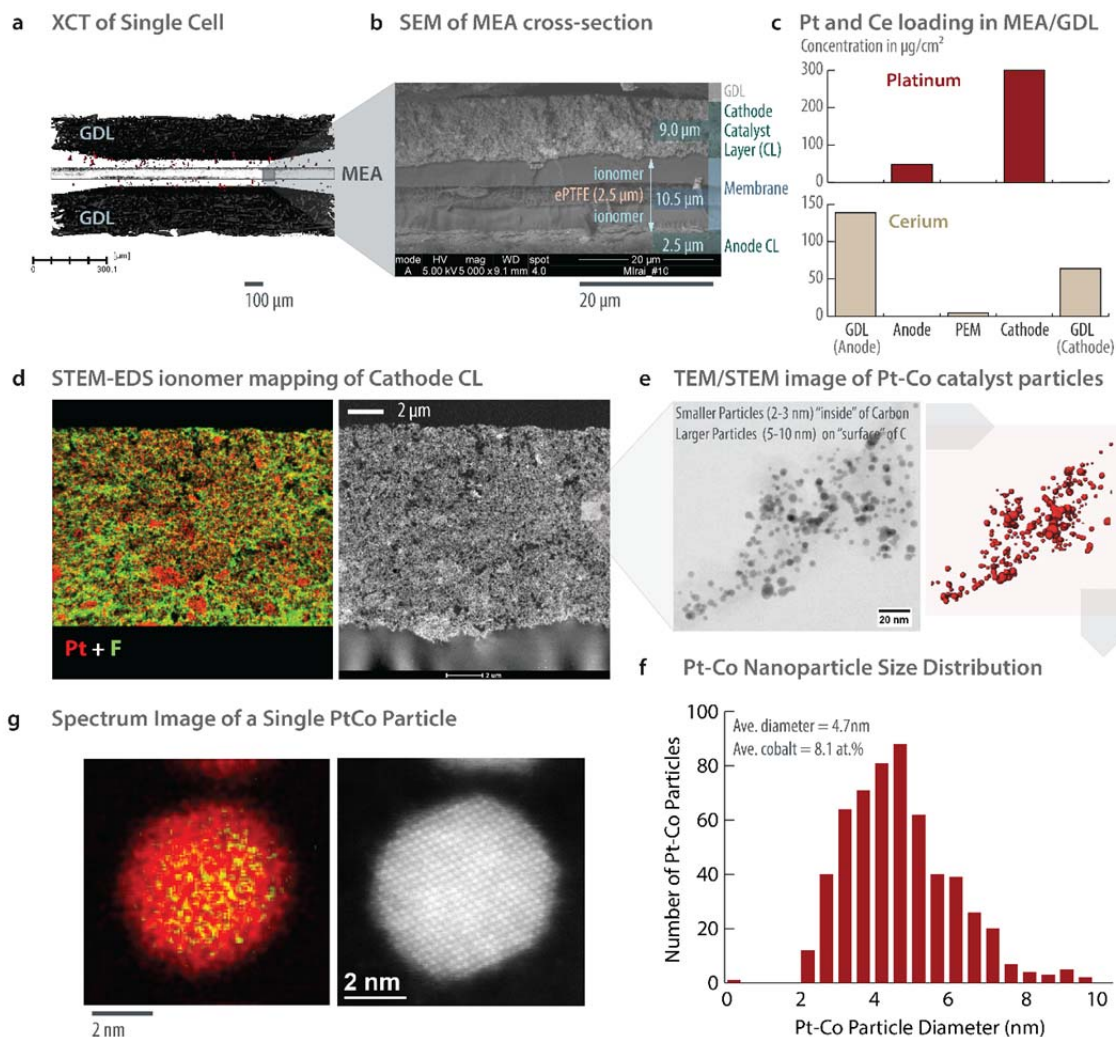function of Pt electrode roughness.Pictorial description of the underlying phenomena (on right).
Data points adapted from ref.[80] (Pt/Vu$_{xx}$), ref.[103] (PtCo HSC - varying water content), ref.[104]
(Pt/Vu), ref.[61] (PtCo/HSC – varying support type), and page 11 of ref.[105] (Pt/Vu – varying EW).
(b) Effect of (Pt) loading on local resistance, R_{nF}, BOL and after 30,000 cycles, calculated from
the breakdown of the measured polarization curves, with breakdown of contribution of R_{nF} to
total resistance. Reproduced from page 19 of ref.[106], 2019 DOE Annual Merit Review.

a   XCT of Single Cell

b   SEM of MEA cross-section

c   Pt and Ce loading in MEA/GDL
Concentration in μg/cm²

d   STEM-EDS ionomer mapping of Cathode CL

e   TEM/STEM image of Pt-Co catalyst particles

f   Pt-Co Nanoparticle Size Distribution

g   Spectrum Image of a Single PtCo Particle

868

869

870   **Figure 7. Current state-of-the-art materials used in passenger fuel cell vehicles and their**
871   **characterization results.** Summary of materials used in a single cell from the 370 cell, 114kW
872   PEMFC stack of a Toyota Mirai FCEV; characterization performed by the FC-PAD consortium.
873   (a) X-ray computed tomography (XCT) of the MEA and GDL showing thickness of GDL and
874   MEA, (b) Scanning electron microscopy (SEM) of the MEA cross-section showing thickness of
875   membrane and catalyst layers, (c) Pt and Ce loadings in cell components determined by X-ray
876   fluorescence, (d) Scanning transmission electron microscopy and energy dispersive X-ray
877   spectroscopy (STEM-EDS) of the cathode-catalyst layer showing fluorine (green) elemental
878   map, representing ionomer distribution, overlaid on platinum (red), (e) STEM tomography
879   showing distribution of Pt-Co particles over and within the carbon support, (f) size distribution
880   of cathode catalyst particles, and (g) STEM-EDS map of individual Pt-Co nanoparticle showing
881   alloy core covered with a Pt-rich shell. Panels adapted from pages 23-30 of ref.[107], 2018 DOE
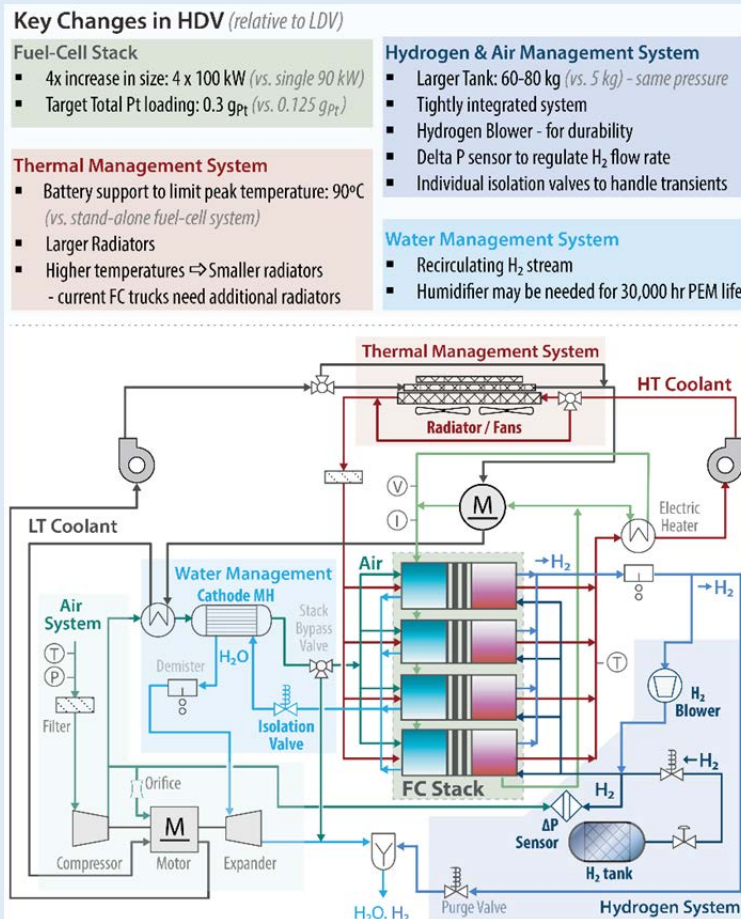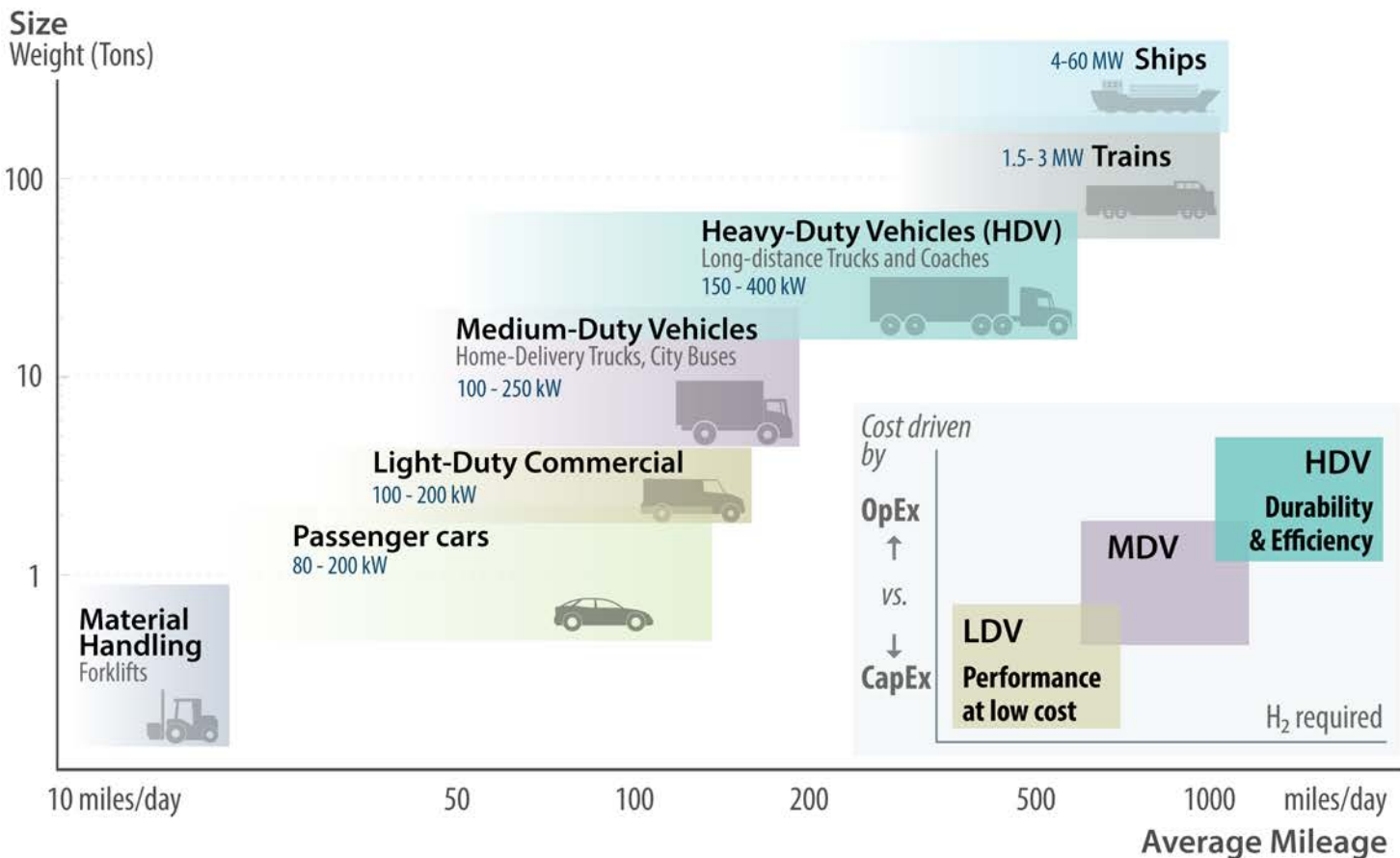882   Annual Merit Review

883

884

26

885

886 **Box:**

887 Title: Conceptual design for next-generation PEMFC system for HDVs

888 While the blueprint for HDV systems can be derived from the layouts for LDVs, the balance of
889 plant components in HDVs have some significant differences to accommodate the larger number
890 of stacks and to aid with the increased efficiency and durability requirements. The conceptual
891 system is built around four 100-kWe gross stacks, standardized to promote manufacturing at
892 volumes necessary for economy of scale. The air management system incorporates a single
893 turbo compressor patterned after superchargers for long-haul trucks, but is driven by a motor
894 with a motor-controller and an optional expander to reduce the parasitic power. The fuel-
895 management system consists of a single recirculation blower, demister, and valves for regulating
896 the inlet pressure of fresh hydrogen. The water-management system includes a cathode
897 membrane humidifier to ensure longer membrane lifetimes by avoiding hot dry operations. The
898 thermal-management system consists of a low-temperature (LT) circuit for cooling the
899 compressor discharge air and a high-temperature (HT) circuit for the stack coolant. The overall
900 system incorporates minimum controls for isolating the anode and cathode during startup and
901 shutdown and for depleting H_2 and O_2 to avoid the formation of H_2/O_2 fronts at the anode that
902 lead to damaging high internal cathode potentials (i.e., cell reversal). Adapted from page 16 of
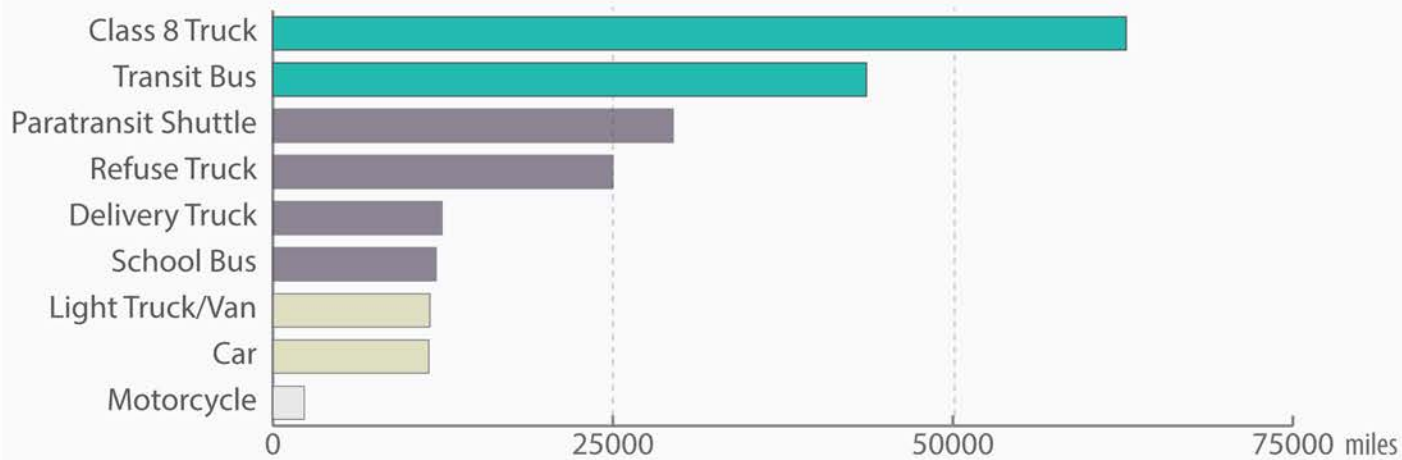903 ref.[29], 2020 DOE Annual Merit Review

904

905

a Hydrogen Fuel Cell Diversity in Transportation

Size
Weight (Tons)

4-60 MW **Ships**

1.5- 3 MW **Trains**

Heavy-Duty Vehicles (HDV)
Long-distance Trucks and Coaches
150 - 400 kW

Medium-Duty Vehicles
Home-Delivery Trucks, City Buses
100 - 250 kW

Light-Duty Commercial
100 - 200 kW

Passenger cars
80 - 200 kW

Material Handling
Forklifts

100

10

1

Cost driven by

OpEx
↑
vs.
↓
CapEx

HDV
Durability & Efficiency

MDV

LDV
Performance at low cost

H₂ required

10 miles/day   50   100   200   500   1000   miles/day

Average Mileage

---

b Average Annual Vehicle Miles Traveled by Major Vehicle Category

- Class 8 Truck
- Transit Bus
- Paratransit Shuttle
- Refuse Truck
- Delivery Truck
- School Bus
- Light Truck/Van
- Car
- Motorcycle

0   25000   50000   75000 miles

---

c

Potential Hydrogen demand market size

⬤ 1 million metric tons of H₂

2050
2030
Light-duty Passenger Vehicles
including pickup trucks
SUVs, crossovers, taxis

2050
2030
Medium/heavy-duty Trucks
vans/light commercial vehicles
captive trucks in ports & mines

FCEVs on the road in US
(LDV+HDV)

5,300,000

200,000
50,000

2030
Broad Rollout

2025
Diversification
Near-term

H₂ Fueling Stations in US

5,600

580
110

a

Cost ($/kW)

100

$80/kW
HDV
$60/kW

$40/kW
LDV
$30/kW

0

Interim 2030 · Ultimate 2050

Efficiency (peak)

80%

HDV
68% → 72%
65% → 70%
LDV

50%

Interim 2030 · Ultimate 2050

System Lifetime (hours)

40,000

HDV
25,000 → 30,000

LDV
5,000 → 8,000

0

Interim 2030 · Ultimate 2050

b

Fuel-Cell Vehicles Durability Targets
in miles

1 m miles · HDV
LDV

0.5 m

150k

Truck · Bus · Car

c

	Interim	Ultimate			
Truck		HDV (Targets)			Fuel Cells
10 – 12 years					
Locomotive					Diesel Engines
10 years or 750k miles					
Ferry Boat					
center section overhaul	intermediate overhaul			major overhaul	

0k · 20k · 40k · 60k · 80k hours

a

b

Fuel Cell Components: "design space" for heavy duty stack with materials of the future

Bipolar plate Current collector with Gas flow channels

Gas Diffusion Layer (GDL) Micro-porous carbon-based diffusion media

Membrane-Electrode Assembly (MEA)

Gas Diffusion Layer (GDL)

Anode Catalyst Layer (ACL)
Proton-Exchange Membrane (PEM)
Cathode Catalyst Layer (CCL)

Heteregeneous Nano- and meso-porous Catalyst Structure

Anode $H_2 \rightarrow 2e^- + 2H^+$

PEM H^+ and H_2O transport

Cathode $4H^+ + 4e^- + O_2 \rightarrow 2H_2O$

CCL

PEM

O$_2$

thin film ionomer

H^+ $\rightarrow$ H_2O

Platinum

e^- Carbon

Bipolar Plates
Material (Ti, SS, Al)
Corrosion coatings
Cost and Weight

GDL
Porosity
Thickness
Carbon Type
Ionomer Coating

PEM
Ionomer Chemistry
Additives, Reinforcement
Temperature & RH dependence
Performance & Durability

Electrodes
Nano- and meso-porous structure
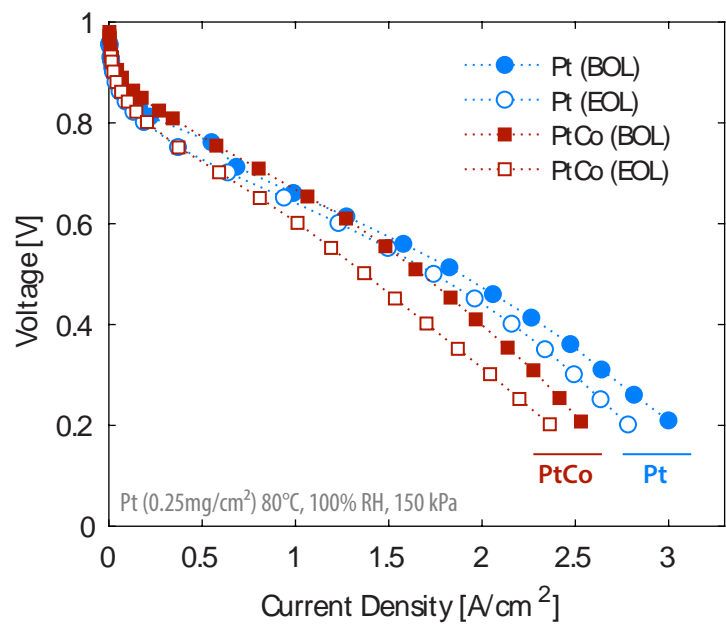Ionomer:Carbon (I:C) ratio, Pt loading
Ink Formulation, Casting and Processing
Conditioning for Performance & Durability

Catalyst, Support, and Ionomers
Carbon type and structure (porosity, graphitization)
Ionomer-Electrocatalyst interactions, ionomer chemistry
Nanoparticle catalyst (alloying, ordering, monodispersity)

a

Local Transport Resistance, R_{nF} [s/cm]

Electrode Roughness, f_{Pt} [cm$^2_{Pt}$/cm$^2_{MEA}$]

ink solvent effects
Varying ink solvent composition and
alcohol-water ratio impact aggregation

PtCo/HSC

Pt/Vu$_{TKK}$

support effects
Varying primary pore geometry/volume
changes electrochemical accessibility

a

b

f

ionomer effect
Varying fraction of
ionic sites (charges)

Pt/Vu

Pt/Vu

▽ Pt/Vu
● PtCo/HSC - *Varying Water Content*
■ PtCo/HSC - *Varying Support Type*
▲ Pt/Vu$_{TKK}$ - *Varying ink solvent composition*
☐ Pt/Vu - *Varying Equivalent Weight (EW)*

INK SOLVENT
alcohol-rich solvent
water-rich solvent

SUPPORT TYPE
Solid
Accessible
Porous
Limited Accessibility

IONOMER CHEMISTRY
Low EW = less ionic sites
High EW = more ionic sites

b

Local Transport Resistance, R_{nF} [s/cm]

After 30k Cycles

Beginning of Life (BOL)

Pt Loading [mg/cm^2]

Ratio of R_{nF} to Total Resistance %

Pt Loading :

0.05

0.10
0.15

BOL   30k Cycles

a   XCT of Single Cell

GDL

GDL

300.1 [μm]

100 μm

b   SEM of MEA cross-section

MEA

GDL
Cathode Catalyst Layer (CL)   9.0 μm
ionomer
ePTFE (2.5 μm)   Membrane   10.5 μm
ionomer
Anode CL   2.5 μm

| mode | HV | mag | WD | spot | 20 μm |
| A | 5.00 kV | 5 000 x | 9.1 mm | 4.0 | MIrai #10 |

20 μm

c   Pt and Ce loading in MEA/GDL

Concentration in μg/cm^2

Platinum

Cerium

GDL (Anode)   Anode   PEM   Cathode   GDL (Cathode)

d   STEM-EDS ionomer mapping of Cathode CL

2 μm

Pt + **F**

2 μm

e   TEM/STEM image of Pt-Co catalyst particles

Smaller Particles (2-3 nm) "inside" of Carbon
Larger Particles (5-10 nm) on "surface" of C

20 nm

f   Pt-Co Nanoparticle Size Distribution

Ave. diameter = 4.7nm
Ave. cobalt = 8.1 at.%

Number of Pt-Co Particles

Pt-Co Particle Diameter (nm)

g   Spectrum Image of a Single PtCo Particle

2 nm

2 nm

Key Changes in HDV *(relative to LDV)*

Fuel-Cell Stack
- 4x increase in size: 4 x 100 kW *(vs. single 90 kW)*
- Target Total Pt loading: 0.3 g_{Pt} *(vs. 0.125 g_{Pt})*

Thermal Management System
- Battery support to limit peak temperature: 90ºC *(vs. stand-alone fuel-cell system)*
- Larger Radiators
- Higher temperatures ⇨ Smaller radiators
  - current FC trucks need additional radiators

Hydrogen & Air Management System
- Larger Tank: 60-80 kg *(vs. 5 kg) - same pressure*
- Tightly integrated system
- Hydrogen Blower - for durability
- Delta P sensor to regulate H_2 flow rate
- Individual isolation valves to handle transients

Water Management System
- Recirculating H_2 stream
- Humidifier may be needed for 30,000 hr PEM life